



HAL
open science

Novel 8-nitroquinolin-2(1 H)-ones as NTR-bioactivated antikinoplastid molecules: Synthesis, electrochemical and SAR study

Julien Pedron, Clotilde Boudot, Sébastien Hutter, Sandra Bourgeade-Delmas, Jean-Luc Stigliani, Alix Sournia-Saquet, Moreau Alain, Elisa Boutet-Robinet, Lucie Paloque, Emmanuelle Mothes-Martin, et al.

► To cite this version:

Julien Pedron, Clotilde Boudot, Sébastien Hutter, Sandra Bourgeade-Delmas, Jean-Luc Stigliani, et al.. Novel 8-nitroquinolin-2(1 H)-ones as NTR-bioactivated antikinoplastid molecules: Synthesis, electrochemical and SAR study. *European Journal of Medicinal Chemistry*, 2018, 155, pp.135 - 152. 10.1016/j.ejmech.2018.06.001 . hal-01888465

HAL Id: hal-01888465

<https://unilim.hal.science/hal-01888465v1>

Submitted on 7 Nov 2024

HAL is a multi-disciplinary open access archive for the deposit and dissemination of scientific research documents, whether they are published or not. The documents may come from teaching and research institutions in France or abroad, or from public or private research centers.

L'archive ouverte pluridisciplinaire **HAL**, est destinée au dépôt et à la diffusion de documents scientifiques de niveau recherche, publiés ou non, émanant des établissements d'enseignement et de recherche français ou étrangers, des laboratoires publics ou privés.

Published in final edited form as:

Eur J Med Chem. 2018 July 15; 155: 135–152. doi:10.1016/j.ejmech.2018.06.001.

Novel 8-nitroquinolin-2(1*H*)-ones as NTR-bioactivated antiketoplastid molecules: Synthesis, electrochemical and SAR study

Julien Pedron^a, Clotilde Boudot^b, Sébastien Hutter^c, Sandra Bourgeade-Delmas^d, Jean-Luc Stigliani^a, Alix Sournia-Saquet^a, Alain Moreau^a, Elisa Boutet-Robinet^e, Lucie Paloque^a, Emmanuelle Mothes^a, Michèle Laget^f, Laure Vendier^a, Geneviève Pratiel^a, Susan Wyllie^g, Alan Fairlamb^g, Nadine Azas^c, Bertrand Courtioux^b, Alexis Valentin^d, Pierre Verhaeghe^{a,*}

^aLCC-CNRS Université de Toulouse, CNRS, UPS, Toulouse, France

^bUniversité de Limoges, UMR INSERM 1094, Neuroépidémiologie Tropicale, Faculté de Pharmacie, 2 rue du Dr Marcland, 87025, Limoges, France

^cIHU Méditerranée Infection, équipe VITROME « Vecteurs, Infections Tropicales et Méditerranéennes, 19-21 boulevard Jean Moulin, 13385, Marseille Cedex 05, France

^dUMR 152 PharmaDev, Université de Toulouse, IRD, UPS, Toulouse, France

^eToxalim (Research Centre in Food Toxicology), Université de Toulouse, INRA, ENVT, INP-Purpan, UPS, Toulouse, France

^fUMR MD1, U1261, AMU, INSERM, SSA, IRBA, MCT, Marseille, France

^gUniversity of Dundee, School of Life Sciences, Division of Biological Chemistry and Drug Discovery, Dow Street, Dundee, DD1 5EH, Scotland, United Kingdom

Abstract

To study the antiparasitic 8-nitroquinolin-2(1*H*)-one pharmacophore, a series of 31 derivatives was synthesized in 1–5 steps and evaluated *in vitro* against both *Leishmania infantum* and *Trypanosoma brucei brucei*. In parallel, the reduction potential of all molecules was measured by cyclic voltammetry. Structure-activity relationships first indicated that antileishmanial activity depends on an intramolecular hydrogen bond (described by X-ray diffraction) between the lactam function and the nitro group, which is responsible for an important shift of the redox potential (+0.3 V in comparison with 8-nitroquinoline). With the assistance of computational chemistry, a set of derivatives presenting a large range of redox potentials (from –1.1 to –0.45 V) was designed and provided a list of suitable molecules to be synthesized and tested. This approach highlighted that, in this series, only substrates with a redox potential above –0.6 V display activity toward *L. infantum*. Nevertheless, such relation between redox potentials and *in vitro* antiparasitic activities was not observed in *T. b. brucei*. Compound **22** is a new hit compound in the series, displaying both antileishmanial and antitrypanosomal activity along with a low cytotoxicity on the human

*Corresponding author. pierre.verhaeghe@lcc-toulouse.fr, pierre.verhaeghe@univtlse3.fr (P. Verhaeghe).

Notes

The authors declare no competing financial interest.

HepG2 cell line. Compound **22** is selectively bioactivated by the type 1 nitroreductases (NTR1) of *L. donovani* and *T. brucei brucei*. Moreover, despite being mutagenic in the Ames test, as most of nitroaromatic derivatives, compound **22** was not genotoxic in the comet assay. Preliminary *in vitro* pharmacokinetic parameters were finally determined and pointed out a good *in vitro* microsomal stability (half-life > 40 min) and a 92% binding to human albumin.

Keywords

Anti-kinetoplastids; *Leishmania*; *Trypanosoma*; 8-Nitroquinolin-2(1*H*)-one; Nitroreductases; Electrochemistry

1 Introduction

Kinetoplastids are protozoan parasites responsible for deadly mammalian infections; *Leishmania* spp and *Trypanosoma* spp being the two main genera encountered in human pathology. These parasites are transmitted to their mammalian hosts by the bite of specific insect vectors. Among the *Leishmania* genus, *L. donovani* and *L. infantum* are the two most important species responsible for visceral leishmaniasis (VL), the most severe and often lethal clinical form of the disease. Briefly, VL occurs in humans after the bite of a sandfly (*Phlebotominae*) which injects the metacyclic flagellated promastigote stage of the parasite into the skin. Parasites are then phagocytized by macrophages and other types of mononuclear phagocytic cells where they transform into the amastigote stage and multiply, bypassing the immune system of the host. Infected cells disseminate in many tissues and organs such as lymph nodes, liver, spleen and bone marrow, leading to death [1]. In the *Trypanosoma* genus, in addition to *T. cruzi* species, causing Chagas disease in South and Central America, the *T. brucei* species (*T. brucei gambiense* or *T. brucei rhodesiense*) are responsible for Human African Trypanosomiasis (HAT), also called “sleeping sickness”. During HAT, the flagellated trypomastigote stage of the parasites penetrates into the blood stream *via* the bite of a “tsetse fly” and disseminates into the whole organism. In a first step of the disease, headaches, anemia, joint pain and various organ damage occur. Then, in a second step, the parasites invade the central nervous system, causing various neurological changes such as sleeping disorders (responsible for the name of the disease), abnormal tone and mobility, ataxia, psychiatric disorders, seizures, coma and finally, death [2].

It is important to note that all these kinetoplastid infections are lethal if untreated and that very few efficient, safe and affordable drugs are available on the market for the low-income infected patients living in developing countries, which makes these parasitic infections belong to the group of “Neglected Tropical Diseases” [3]. Regarding recent epidemiologic data, the WHO indicates that more than 1 billion people are at risk of contracting VL and that 300.000 new cases occur every year, responsible for about 20.000 deaths [4]. Concerning HAT, 61 million people would be at risk of contracting the disease, no clear data being available about HAT mortality [5]. Approved drugs against VL are amphotericin B, miltefosine, antimony V derivatives and pentamidine. The liposomal form of amphotericin B, although being quite efficient, is also very expensive and requires parenteral administration, which makes it unsuitable for treating most of infected patients [6].

Pentamidine and pentavalent antimony derivatives are toxic agents which use is limited by parasitic resistances and poor efficacy [7]. Miltefosine (Fig. 1) remains the only orally available drug, but it is a teratogenic molecule, preventing its use in women of child-bearing age [6]. The context of anti-HAT drugs is quite similar with only one orally available drug [8]. In addition to pentamidine, suramin is used in the treatment of the first stage of the disease, with nifurtimox in combination with eflornithine (NECT, Fig. 1) for treatment of the second (cerebral) stage of HAT. NECT has largely replaced the use of melarsoprol, a highly toxic arsenic-containing drug [2].

Unfortunately, there are very few new chemical entities under clinical trial in 2018 against both VL and HAT [8]. In this worrying context, there is a critical need to identify new active molecules and, as observed in the field of tuberculosis, various nitroheterocycles such as delamanid and fexinidazole are re-emerging as key anti-infective molecules [9,10]. Fexinidazole (Fig. 1) is a 5-nitroimidazole derivative that was first evaluated against visceral leishmaniasis in a phase II clinical trial. Although not sufficiently efficient for use as a monotherapy for VL, fexinidazole has now demonstrated efficacy against early and late stages of HAT in a pivotal Phase III clinical trial [11,12]. Fexinidazole is part of these nitroaromatic molecules which are selectively activated by parasitic nitroreductases (NTRs) to generate electrophilic cytotoxic metabolites [13,14]. Unfortunately, no parasitic NTR X-ray structure is available and most classical rational medicinal chemistry approaches cannot be used for the design of new synthetic substrates of these key enzymes. In this context, our group initiated a research around a class of 8-nitroquinoline derivatives with antiparasitic potential [15] and identified an antileishmanial pharmacophore in 2012, corresponding to the 8-nitroquinolin-2(1*H*)-one scaffold (Fig. 1) [16]. Some more recent modulations of the position 4 of this pharmacophore failed to achieve more active derivatives [17,18]. Here, we present a comprehensive study of the structure-activity relationships of this pharmacophore, especially focusing on the modulation of the redox potentials. Thirty one pharmacophore derivatives, substituted at positions 3, 4, 5, 6 and 7, were synthesized and their *in vitro* cytotoxicity and activities against *L. infantum* (axenic amastigotes), and *T. brucei brucei* (trypomastigotes) were first determined. The original pharmacophore possessed poor antitrypanosomal activity, whereas a new derivative (compound **22**) was identified, active against all tested kinetoplastids (*L. donovani* promastigotes, *L. donovani* intramacrophage amastigotes, *L. infantum* axenic amastigotes and *T. brucei brucei* trypomastigotes). The antileishmanial mechanism of action of this new hit-compound will be discussed along with its mutagenicity and genotoxicity, a key aspect concerning nitroaromatic compounds. Finally, two preliminary *in vitro* pharmacokinetic properties were measured and appear favorable for further development of this anti-kinetoplastid pharmacophore.

2 Results and discussion

2.1 Chemistry

Thirty one derivatives of the initial 8-nitroquinolin-2-(1*H*)-one pharmacophore, including 14 original ones, were prepared. As presented in Scheme 1, compounds **1–5** were obtained by classical nitration, cyclo-condensation or *N*-acetylation reactions. Nitration at position 8 of 2-chloro-4-methylquinoline afforded **6** whose chloroimine moiety reacted with perchloric

acid to generate the corresponding lactam **7**, according to a simple and efficient previously reported procedure [19]. Bromination of **7** with *N*-bromosuccinimide led to the bromomethyl derivative **8** which was reacted with sodium hydroxide to generate hydroxymethyl derivative **9**. From bromomethyl **8**, by reacting with an amine, it was also possible to access to **10** and its deprotected counterpart **11**. From 2,4-dibromoquinoline, by a sequential nitration/lactamisation procedure, **12** and **13** were obtained in good yields.

As presented in Scheme 2, the 2-chloroquinoline was the main substrate used in this work. It was first reacted with perchloric acid to generate lactam **14** which was either nitrated at position 6, to afford compound **15** or *N*-methylated with methyl iodide, to afford **16** in good yields. The nitration of 2-chloroquinoline mainly led to the 2 position isomers **17** and **18** which were transformed into the corresponding lactams **19** and **20**. Compound **20** was either *O*-methylated with methyl iodide, forming **21**, or selectively halogenated at position 3 by refluxing in HBr or HCl in the presence of sodium bromate or sodium chlorate, to generate derivatives **22** and **23**. Note that this specific halogenation procedure (*in situ* Br₂ or Cl₂ formation and reaction in refluxing aqueous medium), reported by O'Brien and co-workers [20], is the only one allowing selective halogenation at position 3 among many others that were tested. The 3-brominated derivative **22** reacted with methyl iodide to form *O*-methylated derivative **24** or was reduced into the amino-derivative **25** by using SnCl₂.

Finally, as presented in Scheme 3, we also used another synthetic pathway allowing the preparation of 8-nitroquinolinone derivatives bearing substituents on the benzene moiety. This strategy was reported by Zaragoza and co-workers [21]. First, commercial 3,3'-diethoxyethylpropionate was saponified into the corresponding carboxylic acid which was then reacted with SOCl₂ to form the acyl chloride. This acyl chloride was then reacted with various *ortho*-nitroanilines, to give the corresponding *N*-acylated products which were not isolated. In a final step, cyclization was operated in 98% H₂SO₄, giving the expected products **26**–**31**. The reaction yields are moderate when using 2-nitroanilines substituted at position 3 or 5 by electron donating groups but turn to be very low when using 2-nitroanilines substituted at position 4 by the same groups.

3 Compound evaluation

3.1 *In vitro* activity against *L. infantum* and *T. brucei brucei*: importance of the redox potential

All synthesized molecules were screened *in vitro* toward both *L. infantum* axenic amastigotes and *T. brucei brucei* trypomastigotes and compared with commercial reference drugs (amphotericin B and miltefosine against *L. infantum*, suramin and eflornithine against *T. brucei*) along with drug-candidate fexinidazole (Table 1). To assess antiparasitic selectivity, the cytotoxicity of all compounds was also measured on the HepG2 human cell line, using doxorubicin as control. In parallel the LogP of all compounds were calculated and the reduction potentials were measured by cyclic voltammetry in DMSO. The redox potentials measured correspond to a one electron reduction/oxidation regarding the redox couple nitro group/anion radical. Only one new hit compound (**22**) was evaluated in greater depth, as the best compound in the series regarding both activity and selectivity.

Globally, apart from molecule **24**, all synthesized compounds were soluble in aqueous medium and could be evaluated *in vitro*. Out of the 31 tested compounds, none appeared cytotoxic on the HepG2 cell line, nine were active toward *L. infantum* axenic amastigotes (7 μM IC_{50} 25 μM) and thirteen were active against *T. brucei brucei* trypomastigotes (2 μM IC_{50} 25 μM), molecule **24** being excluded from the analysis because of its lack of solubility. As a first approach, we wanted to see if there was a relationship between activity and lipophilicity. Computed LogP, ranging from 1.15 to 2.5 did not show any correlation, active molecules presenting either low (compound **2**) or high (compound **22**) LogP values.

We then explored the structure-activity relationships (SARs) of the pharmacophore by focusing on the influence of the redox potentials toward the activity against *L. infantum*. Indeed, on the basis that this nitroaromatic pharmacophore could be the substrate of parasitic nitroreductases, it first appeared important to understand which chemical criteria would make this pharmacophore suitable for being efficiently reduced into cytotoxic metabolites. The basic redox potential value of 8-nitroquinoline 1 (−0.84 V) and nitrobenzene (−0.85 V) are quite low and do not seem suitable for the catalytic capabilities of the parasitic nitroreductases (Fig. 2). On the contrary, when the lactam function is combined with the presence of a nitro group at position 8 (initial hit), a significant increase in the value of the redox potential, up to −0.54 V, is observed and the molecule turns active. When keeping the lactam function while moving the nitro group at position 6 or 5 (compounds **15** and **19**), redox potentials become lower and the IC_{50} values of the molecules increased, resulting in a loss of activity against *L. infantum*. The same effect is noted with inactive *O*-methylated analog (compound **21**), which redox potential drastically fell to −0.93 V (Fig. 2). Finally, adding an amide function in the *ortho* position of the nitrogroup (compounds **3** and **5**) did not provide an optimal value of redox potential (−0.68 V and −0.86 V, respectively) resulting in poor antileishmanial activity of the compounds. Thus the 8-nitroquinolin-2-(1*H*)-one scaffold definitely appears to be the antileishmanial pharmacophore. Besides, as presented in the X-ray diffraction structures (Fig. 3), this pharmacophore presents a noticeable intramolecular hydrogen bond between the lactam function and the nitro group at position 8, responsible for a +0.3 V increase in redox potentials, allowing antileishmanial activity. Nevertheless, molecules **26** and **30**, which present the same redox potential, do not have the same antileishmanial activity (**26** being moderately active and **30** being inactive). By examining their LogP values (respectively 2.05 and 1.38) it could be hypothesized that antileishmanial activity depends on a compromise between redox potential values and lipophilicity.

Contrary to what was observed in *Leishmania*, the anti-trypansomal activity did not depend on the redox potential values in the studied series, active molecules presenting either low (compound **15**) or high (compound **22**) redox potential values. It could be hypothesized that the enzymatic capabilities of the *T. brucei* NTR may be compatible with a broader spectrum of redox potentials than the ones of *L. donovani* NTR.

Optimization of redox potentials: computational and *in vitro* studies.

From this point, we investigated the antileishmanial pharma-comodulation of 8-nitroquinolin-2(1*H*)-one by introducing various substituents (or heteroatoms) at all positions

of the scaffold and compared the effect of electron-donating and electron withdrawing groups, to gain access to new optimized derivatives. Our goal was to synthesize a series of derivatives presenting a large spectrum of redox potentials, not only to gain a better understanding of the electrochemical process, but also to define as precisely as possible the lowest redox potential value compatible with activity in the series. For that purpose instead of synthesizing molecules randomly, we used ab initio calculations to estimate the redox potential values of many hypothetical derivatives. Previous studies about the computation of reduction potentials of nitroaromatic derivatives showed that the results are very sensitive to the basis set applied. Diffuse s and p-type functions, combined with polarization functions were shown to be important for electron affinity calculations of nitrobenzenes [22,23]. Because accurate results were obtained with the Pople's 6-311++G basis set on several molecules for which computed potentials were compared to experimental ones, the 6-311++G (2 d, 2p) basis set was selected as a good compromise between accuracy and computational cost for reduction potential calculations. The hybrid M06-2x density functional was chosen for its accuracy to compute thermochemical parameters. The standard redox potentials were computed with the Faraday's law (see equation (1) in the experimental section) from the free energy of the one-electron reduction. Fig. 4 shows the correlation between the experimental and theoretical redox potentials. It can be seen that the slope of the correlation is close to 1.00 and the correlation coefficient (r) is 0.97. Therefore, this model was very efficient for predicting the standard redox potentials and was used to select the most appropriate compounds to be synthesized and evaluated.

The studied series was completed with 11 derivatives of the pharmacophore presenting redox potentials ranging from -0.75 V to -0.45 V. Fig. 5 shows that introducing a heteroatom at position 4 of the scaffold (quinoxaline analog **2**) or a halogen atom at position 3 (compounds **22** and **23**) increased the redox potential values by about $+0.1$ V, the corresponding molecules being active against *L. infantum*. When modifying the pyridinone moiety by introducing a methyl group or a bromine atom at position 4 (compounds **7** and **13**, respectively), the redox potential almost remained unchanged and the molecules were active. By substituting the benzene moiety with a methyl group at position 5 or 6 (compounds **26** and **27**), the redox potentials decreased slightly (down to -0.58 V) and the molecules, were less efficient ($IC_{50} \approx 25$ μ M). Compounds bearing a methoxy group at positions 5, 6 or 7 (compounds **29–31**) or a methyl group at position 7 (compound **28**) showed lower redox potentials, varying from -0.58 V to -0.75 V, and were totally inactive ($IC_{50} > 100$ μ M). Thus, in this series, it can be noted that the optimal redox potential value to target in order to obtain antileishmanial activity is -0.5 V and that molecules whose redox potential is positioned below -0.6 V lost all activity.

Among all synthesized compounds, derivative **22** was highlighted as a new hit (Table 1). It is not only active against *L. infantum* ($IC_{50} = 7.1$ μ M), but also against *T. brucei brucei* ($IC_{50} = 1.9$ μ M), which was not the case of the initial hit, displaying modest activity ($IC_{50} = 23.4$ μ M) toward the latter parasite. For comparison with the anti-leishmanial reference drugs, hit compound **22** appears much less active than amphotericin B and about 10 times less active than miltefosine (with equivalent cytotoxicity). Regarding anti-HAT drugs, hit compound **22** appears much less active than suramin, but more active than eflornithine. It is also important

to compare hit molecule **22** with drug candidate fexinidazole, as they both belong to the nitroaromatic family: **22** is about 2 times more cytotoxic and, depending on the parasite, between 2 and 5 times less active than this drug candidate, which remains interesting for a hit-compound. It was then necessary to evaluate the *in vitro* activity of **22** against the amastigote stage of *Leishmania* in an intramacrophage model, closer to the *in vivo* situation. As presented in Table 2, the test was done on *L. donovani*, the other species responsible for VL. Hit molecule **22**, displays a low cytotoxicity on the THP1 macrophage cell line ($CC_{50} = 72 \mu\text{M}$) and is about 3 times less active ($IC_{50} = 18 \mu\text{M}$) on this intramacrophage amastigote *in vitro* model than miltefosine ($IC_{50} = 5.4 \mu\text{M}$). Fexinidazole is not active on the intramacrophage amastigote stage ($IC_{50} > 50 \mu\text{M}$) as it first needs to be metabolized into a sulfone derivative [24]. Finally, as expected, compound 14 (non nitrated) and **25** (8-amino derivative), negative controls deriving from hit **22**, did not display any antiparasitic activity.

In order to assess whether this compound series was a substrate of parasitic NTRs, the hit compound **22** was assayed against a wild type strain of *L. donovani* promastigotes and two strains overexpressing NTR1 [25] and NTR2 [26], respectively (Table 2). Compound **22** was ten times more effective against the strain overexpressing NTR1 ($IC_{50} = 0.47 \mu\text{M}$) vs WT and NTR2 strains, indicating that it is selectively bioactivated by NTR1 of *L. donovani*. Interestingly, this is the same type 1 nitroreductase that bioactivates fexinidazole and its metabolites [25]. Following the same approach in *T. brucei brucei*, it was also demonstrated that type 1 NTR, the unique NTR enzyme expressed in this parasite, was responsible for the bioactivation of **22** (Table 2).

Nitroaromatic drugs are often suspected to be mutagenic or genotoxic, which has considerably limited the development of such derivatives in the past decades [27]. The most famous *in vitro* test used for evaluating mutagenicity is the Ames test, using *Salmonella typhimurium* strains. Nevertheless, considering that *Salmonella* bacteria possess nitroreductases [28], the Ames test is usually positive when evaluating nitroaromatics, with no real predicting character for humans, considering that there are no NTRs in mammalian cells and that most of nitroaromatic derivatives only exert a genotoxic character after being bioactivated into reduced metabolites [27]. For that reason, it is nowadays accepted that the comet assay or the micronucleus assay are better *in vitro* tools for evaluating the potential genotoxicity of nitroaromatics [27]. Indeed, metronidazole, one of the most famous anti-infective nitroheterocycles on the market, is mutagenic in the Ames test, but not genotoxic in the comet assay [29] and fexinidazole is not genotoxic in the micronucleus assay despite being mutagenic in the Ames test [24]. Regarding compound **22**, the Ames test (in metabolizing conditions) and the comet assay were done in parallel and revealed that, although being mutagenic in the Ames test (Table 3) at 0.25 or 2.5 mM, compound **22** was not genotoxic in the comet assay after 2 or 72 h of exposure, at 1, 10, 20 or 40 μM (Fig. 6), concentrations chosen from the HepG2 $CC_{10\%}$ (40 μM). This lack of genotoxicity is a key point when thinking about further development of this pharmacophore. Finally, preliminary *in vitro* pharmacokinetic evaluations were done with compound **22** (Table 2). It presented a very good microsomal stability ($T_{1/2} > 40 \text{ min}$) and had a strong, but not extreme binding to human albumin (92%), in relation with the relatively high value of its calculated $\log P$ (= 2.36).

4 Conclusion

Starting from the previously identified 8-nitroquinolin-2(1*H*)-one antileishmanial pharmacophore, an electrochemistry-guided SAR study revealed that an intramolecular hydrogen bond between the lactam ring and the nitro group is responsible for a +0.3 V increase in the redox potential value (compared with 8-nitroquinoline) resulting in improved antileishmanial activity. A computational model allowed the prediction of the redox potential values of any derivative belonging to this series, and we synthesized a set of derivatives presenting a large range of redox potential values. Then, it was highlighted that, to be active, molecules belonging to this series must display a redox potential value of about -0.5 V and that molecules with a redox potential below -0.6 V were inactive. By introducing electron-withdrawing groups on the pyridone moiety of the scaffold, a new original hit compound was found: 22. Presenting a low cytotoxicity on the human HepG2 cell line ($CC_{50} = 92 \mu\text{M}$), it displays activity toward *L. infantum* axenic amastigotes ($IC_{50} = 7.1 \mu\text{M}$), *L. donovani* promastigotes ($IC_{50} = 5.9 \mu\text{M}$) and *L. donovani* intramacrophagic amastigotes ($IC_{50} = 18 \mu\text{M}$), but also toward *T. brucei brucei* ($IC_{50} = 1.9 \mu\text{M}$). Moreover, we demonstrated that 22 was not genotoxic in the comet assay and that it was selectively bioactivated by the mitochondrial NTR1 of *L. donovani* and *T. brucei brucei*. This whole study, completed with two encouraging preliminary *in vitro* pharmacokinetic parameters (good microsomal stability and 92% binding to human albumin) now opens the way to the rational conception, guided with E° values, of new efficient, selective and safe NTR1 bioactivated 8-nitroquinolin-2(1*H*)-ones against VL and HAT.

Experimental section

Chemistry

All reagents and solvents were obtained from commercial sources (Fluorochem[®], Sigma-Aldrich[®] or Alfa Aesar[®]) and used as received. The progress of the reactions was monitored by precoated thin layer chromatography (TLC) sheets ALUGRAM[®] SIL G/UV₂₅₄ from Macherey-Nagel and were visualized by ultraviolet light at 254 nm. The NMR ¹H and ¹³C spectra were recorded on a Bruker UltraShield 300 MHz, a Bruker IconNMR 400 MHz, or a Bruker Avance NEO 600 MHz instrument, at the Laboratoire de Chimie de Coordination and data are presented as follows: chemical shifts in parts per million (δ) using tetramethylsilane (TMS) as reference, coupling constant in Hertz (Hz), multiplicity by abbreviations: (s) singlet, (d) doublet, (t) triplet, (q) quartet, (dd) doublets of doublets, (m) multiplet and (br s) broad singlet. Melting points are uncorrected and were measured on a Stuart Melting Point SMP3 instrument. HRMS measurements were done on a GCT Premier Spectrometer (DCI, CH₄, HRMS) or Xevo G2 QTOF (Waters, ESI+, HRMS) instrument at the Université Paul Sabatier, Toulouse. Microwave reactions were realized in a CEM Discover[®] microwave reactor. All products were purified by chromatography columns and then recrystallized. Purity of the products was determined by ¹H NMR.

General procedure for the preparation of 8-nitroquinoline 1 [30], 7-amino-8-nitroquinoline 4 [31], 2-chloro-4-methyl-8-nitroquinoline 6 [32], 2,4-dibromo-8-nitroquinoline 12 [17], 6-nitroquinolin-2(1*H*)-one 15 [16], 2-chloro-5-nitroquinoline 17 [16] and 2-chloro-8-nitroquinoline 18 [16]:

H₂SO₄ (98%) was added onto 1 equiv. of the quinoline derivatives, cooled with an ice bath. 5 equiv. of 65% HNO₃ were then added dropwise at 0 °C and the reaction mixture was stirred at rt for 1–4 h. The reaction mixture was successively poured into ice, neutralized with NaOH and extracted three times with dichloromethane. The organic layer was washed with water, dried over anhydrous Na₂SO₄ and evaporated *in vacuo*. The crude residue was purified by chromatography on silica gel using adapted eluent and recrystallized if necessary to give compounds 1, 4, 6, 12, 15, 17 and 18.

8-nitroquinoline 1 (C₉H₆N₂O₂) was purified by chromatography on silica gel using dichloromethane as an eluent, separated from its 5-nitro isomer and isolated to yield a pale yellow solid (35%, 2.7 mmol, 470 mg), mp 90 °C (Lit: 90 °C), ¹H NMR (400 MHz, CDCl₃) δ: 7.53–7.66 (m, 2H), 8.04 (d, *J* = 8.0 Hz, 2H), 8.27 (dd, *J* = 1.6 and 8.4 Hz, 1H, H7), 9.70 (dd, *J* = 1.7 and 4.2 Hz, 1H, H2). ¹³C NMR (100 MHz, CDCl₃) δ: 122.8 (CH), 123.8 (CH), 125.3 (CH), 129.0 (C), 132.0 (CH), 136.1 (CH), 139.5 (C), 148.2 (C), 152.6 (CH).

7-amino-8-nitroquinoline 4 (C₉H₇N₃O₂) was purified by chromatography on silica gel using dichloromethane/ethyl acetate (80/20) as an eluent and isolated to yield an orange solid (46%, 0.16 mmol, 30 mg), mp 193 °C (Lit: 194 °C), ¹H NMR (400 MHz, CDCl₃) δ: 5.61 (br s, 2H, NH₂); 7.00 (d, *J* = 9.0 Hz, 1H, H6), 7.28 (dd, 1H, *J* = 4.4 and 8.1 Hz, H3), 7.69 (d, *J* = 9.0 Hz, 1H, H5), 8.00 (dd, 1H, *J* = 1.8 and 8.1 Hz, H4), 8.92 (dd, 1H, *J* = 1.8 and 4.4 Hz, H2). ¹³C NMR (100 MHz, Acetone d₆): 118.90 (CH), 119.8 (CH), 120.9 (C), 131.8 (CH), 135.7 (CH), 139.7 (C), 142.8 (C), 143.1 (C), 151.2 (CH).

2-chloro-4-methyl-8-nitroquinoline 6 (C₁₀H₇ClN₂O₂) was purified by chromatography on silica gel using cyclohexane/acetone (70/30) as an eluent, separated from its 6-nitro isomer, isolated and recrystallized in isopropanol to yield a white solid in (53%, 14.8 mmol, 3.3 g), mp 143 °C (Lit: 142–143 °C), ¹H NMR (400 MHz, CDCl₃) δ: 2.74 (d, *J* = 1.0 Hz, 3H, CH₃), 7.35 (d, *J* = 1.0 Hz, 1H, H3), 7.62–7.66 (m, 1H, H6), 8.00 (dd, *J* = 7.6 and 1.3 Hz, 1H, H5), 8.18 (dd, *J* = 8.4 and 1.3 Hz, 1H, H7). ¹³C NMR (150 MHz, CDCl₃) δ: 18.9 (CH₃), 124.2 (CH), 124.5 (CH), 125.4 (CH), 127.8 (CH), 127.9 (C), 138.9 (C), 147.8 (C), 147.9 (C), 153.2 (C).

2,4-dibromo-8-nitroquinoline 12 (C₉H₄Br₂N₂O₂) was purified by chromatography on silica gel using cyclohexane/acetone (9/1) as an eluent and isolated to yield a white solid (56%, 6 mmol, 2 g), mp 129 °C (Lit: 129 °C), ¹H NMR (400 MHz, CDCl₃) δ: 7.72–7.76 (m, 1H, H6), 8.00 (s, 1H, H3), 8.08 (dd, *J* = 7.6 et 1.4 Hz, 1H, H5), 8.39 (dd, *J* = 8.5 et 1.4 Hz 1H, H7). ¹³C NMR (100 MHz, DMSO) δ: 125.3 (CH), 126.9 (CH), 127.5 (C), 130.9 (CH), 131.0 (CH), 135.0 (C), 139.7 (C), 143.6 (C), 147.5 (C).

6-nitroquinolin-2(1*H*)-one 15 (C₉H₆N₂O₃) was recrystallized in isopropanol to yield a yellow solid (91%, 6.3 mmol, 1.2 g), mp 279 °C (Lit: 279 °C), ¹H NMR (300 MHz, DMSO-*d*₆) δ: 6.68 (d, *J* = 9.8 Hz, 1H, H3), 7.43 (d, *J* = 9.0 Hz, 1H, H8), 8.12 (d, *J* = 9.8 Hz, 1H, H4), 8.33 (dd, *J* = 2.6 and 9.0 Hz, 1H, H7), 8.70 (d, *J* = 2.6 Hz, 1H, H5), 12,3 (br s, 1H, NH). ¹³C NMR (75 MHz, DMSO-*d*₆) δ: 116.3 (CH), 118.7 (C), 124.0 (CH), 124.5 (CH), 125.3 (CH), 140.3 (CH), 141.7 (C), 143.5 (C), 162.1 (C).

2-chloro-5-nitroquinoline 17 (C₉H₅ClN₂O₂) was purified by chromatography on silica gel using cyclohexane/acetone (8/2) as an eluent, isolated and recrystallized in isopropanol to yield a yellow solid (14%, 4.3 mmol, 0.9 g), mp 134 °C (Lit: 133–134 °C), ¹H NMR (300 MHz, CDCl₃) δ: 7.63 (d, *J* = 9.1 Hz, 1H, H4), 7.82–7.87 (m, 1H, H7), 8.34 (dd, *J* = 8.6 and 0.7 Hz, 1H, H8), 8.40 (dd, *J* = 7.6 and 1.2 Hz, 1H, H6), 8.99 (d, *J* = 9.2 Hz, 1H, H3). ¹³C NMR (100 MHz, CDCl₃) δ: 120.1 (C), 125.0 (CH), 125.6 (CH), 129.0 (CH), 135.1 (CH), 135.7 (CH), 145.6 (C), 148.2 (C), 152.6 (C).

2-chloro-8-nitroquinoline 18 (C₉H₅ClN₂O₂) was purified by chromatography on silica gel using cyclohexane/acetone (8/2) as an eluent, isolated and recrystallized in isopropanol to yield a yellow solid (50%, 15.3 mmol, 3.2 g), mp 152 °C (Lit: 152 °C), ¹H NMR (400 MHz, CDCl₃) δ: 7.56 (d, *J* = 8.7 Hz, 1H, H4), 7.65–7.69 (m, 1H, H6), 8.07 (dd, *J* = 8.3 and 1.4 Hz, 1H, H5), 8.11 (dd, *J* = 7.6 and 1.4 Hz, 1H, H7), 8.23 (d, *J* = 8.7 Hz, 1H, H3). ¹³C NMR (150 MHz, CDCl₃) δ: 124.6 (CH), 124.9 (CH), 125.8 (CH), 127.6 (C), 131.8 (CH), 138.6 (CH), 139.0 (C), 147.1 (C), 153.6 (C).

Preparation of 8-nitroquinoxalin-2(1H)-one 2

Ethanol (25 mL) was added onto 1 g of 3-nitro-1,2-phenylenediamine (6.53 mmol, 1 equiv.). 0.6 g of glyoxylic acid monohydrate (6.53 mmol, 1 equiv.) was then added at rt and the reaction mixture was stirred at 80 °C for 6 h. The reaction mixture was poured into water and extracted three times with dichloromethane. The organic layer was washed with water, dried over anhydrous MgSO₄ and evaporated *in vacuo*. The crude residue was purified by chromatography on silica gel using dichloromethane/diethyl ether (80/20) as an eluent. 8-nitroquinoxalin-2 (1H)-one 2 was isolated and recrystallized in acetonitrile to yield an orange solid (46%, 2.98 mmol, 570 mg).

Compound 2 (C₈H₅N₃O₃): mp 162 °C, ¹H NMR (400 MHz, CDCl₃) δ: 7.45–7.50 (m, 1H, H6), 8.25 (dd, *J* = 1.5 and 8.2 Hz, 1H, H5), 8.39 (d, *J* = 2.2 Hz, 1H, H3), 8.55 (dd, *J* = 1.5 and 8.2 Hz, 1H, H7), 11.37 (br s, 1H, NH). ¹³C NMR (100 MHz, CDCl₃) δ: 122.6 (CH), 127.8 (C), 128.0 (CH), 133.1 (C), 133.8 (C), 137.4 (CH), 152.6 (CH), 153.6 (C). HRMS (DCI CH₄) calcd for C₈H₆N₃O₃ [M+H]⁺ 192.0409, found 192.0412.

Preparation of N-(2-Nitrophenyl)-acetamide 3 [33]

Acetic acid (25 mL) was added onto 525 mg of 2-nitroaniline (3.8 mmol, 1 equiv.). The reaction mixture was then stirred at 120 °C and 720 μL of acetic anhydride (7.6 mmol, 2 equiv.) were added dropwise. After 3 h under reflux, the reaction mixture was poured into ice, neutralized with Na₂CO₃ and extracted three times with dichloromethane. The organic layer was washed with water, dried over anhydrous Na₂SO₄ and evaporated *in vacuo*. N-(2-Nitrophenyl)-acetamide 3 was isolated and recrystallized in acetonitrile to yield a yellow solid (87%, 3.3 mmol, 604 mg).

Compound 3 (C₈H₈N₂O₃): mp 93 °C (Lit: 92–94 °C), ¹H NMR (400 MHz, CDCl₃) δ: 2.29 (s, 3H, CH₃), 7.16–7.20 (m, 1H, H4), 7.63–7.67 (m, 1H, H5), 8.21 (dd, *J* = 8.5 and 1.3 Hz, 1H, H6), 8.77 (dd, *J* = 8.6 and 1.3 Hz, 1H, H3), 10.33 (br s, 1H, NH). ¹³C NMR (100 MHz, CDCl₃): 25.60 (CH₃), 122.2 (CH), 123.2 (CH), 125.7 (CH), 134.8 (C), 135.9 (CH), 136.3 (C), 169.0 (C).

Preparation of 7-acetylamino-8-nitroquinoline 5

Glacial acetic acid (20 mL) was added onto 60 mg of 7-amino-8-nitroquinoline (0.32 mmol, 1 equiv.). The reaction mixture was then stirred at 120 °C and 180 µL of acetic anhydride (1.6 mmol, 6 equiv.) were added dropwise. After 24 h under reflux, the reaction mixture was poured into ice, neutralized with K₂CO₃ and extracted three times with dichloromethane. The organic layer was washed with water, dried over anhydrous MgSO₄ and evaporated *in vacuo*. The crude residue was purified by chromatography on silica gel using dichloromethane/ethyl acetate (90/10) as an eluent. 7-acetylamino-8-nitroquinoline 5 was isolated and recrystallized in isopropanol to yield a yellow solid (53%, 0.17 mmol, 39 mg).

Compound 5 (C₁₁H₉N₃O₂): mp 189 °C, ¹H NMR (300 MHz, CDCl₃) δ: 2.28 (s, 3H, CH₃), 7.49 (dd, *J* = 4.3 et 8.3 Hz, 1H, H3), 7.96 (d, 1H, *J* = 9.2 Hz, H 6), 8.19 (dd, *J* = 1.7 et 8.3 Hz, 1H, H4), 8.35 (br s, 1H, NH), 8.54 (d, *J* = 9.2 Hz, 1H, H5), 8.99 (dd, *J* = 1.7 et 4.3 Hz, 1H, H2). ¹³C NMR (150 MHz, CDCl₃) δ: 25.0 (CH₃), 121.7 (CH), 121.9 (CH), 125.2 (C), 127.8 (C), 131.4 (CH), 131.8 (C), 135.8 (CH), 140.3 (C), 152.6 (CH), 168.7 (C). HRMS (DCI CH₄) calcd for C₁₁H₁₀N₃O₂ [M+H]⁺ 232.0722, found 232.0719.

General procedure for the preparation of 4-methyl-8-nitroquinolin-2(1*H*)-one 7 [34], quinolin-2(1*H*)-one 14 [35], 5-nitroquinolin-2 (1*H*)-one 19 [16] and 8-nitroquinolin-2(1*H*)-one 20 [16].

Acetonitrile (25 mL) and 70% perchloric acid solution (25 mL) were added onto 1 equiv. of the quinoline derivatives. The reaction mixture was stirred at 100 °C overnight. The reaction mixture was then poured into ice, neutralized with KOH and extracted twice with dichloromethane. The organic layer was washed with water, dried over anhydrous MgSO₄ and evaporated *in vacuo*. The crude residues were purified by chromatography on silica gel using adapted eluent and recrystallized if necessary to give compounds 7, 14, 19, 20.

4-methyl-8-nitroquinolin-2(1*H*)-one 7 (C₁₀H₈N₂O₃) was isolated and recrystallized in acetonitrile to yield a yellow solid (92%, 11 mmol, 2.2 g), mp 203 °C (Lit: 196 °C), ¹H NMR (400 MHz, DMSO) δ: 3.33 (s, 3H, CH₃), 6.63 (s, 1H, H3), 7.39–7.44 (m, 1H, H6), 8.19 (dd, *J* = 8.0 and 1.3 Hz, 1H, H5), 8.42 (dd, *J* = 8.4 and 1.6 Hz, 1H, H7), 10.98 (br s, 1H, NH). ¹³C NMR (DMSO, 100 MHz) δ: 19.6 (CH₃), 121.6 (CH), 122.0 (CH), 122.6 (C), 127.9 (CH), 133.1 (CH), 133.6 (C) 134.6 (C), 148.9 (C), 161.0 (C). quinolin-2(1*H*)-one 14 (C₉H₇NO) was purified by chromatography on silica gel using dichloromethane/ethyl acetate (8/2) as an eluent and isolated to yield a white solid (74%, 22.7 mmol, 3.3 g), mp 198 °C (Lit: 193 °C), ¹H NMR (400 MHz, CDCl₃) δ: 6.72 (d, *J* = 9.5 Hz, 1H, H3), 7.20–7.25 (m, 1H, H6), 7.40–7.42 (m, 1H, H5), 7.50–7.54 (m, 1H, H7), 7.56–7.58 (m, 1H, H8), 7.82 (d, *J* = 9.5 Hz, 1H, H4), 11.97 (br s, 1H, NH). ¹³C NMR (100 MHz, CDCl₃) δ: 116.3 (CH), 119.9 (C), 121.3 (CH), 122.7 (CH), 127.7 (CH), 130.7 (CH), 138.5 (C), 141.1 (CH), 164.7 (C).

5-nitroquinolin-2(1*H*)-one 19 (C₉H₆N₂O₃) was isolated and recrystallized in acetonitrile to yield a yellow solid (92%, 2.2 mmol, 418 mg), mp 302 °C (Lit: 302 °C), ¹H NMR (400 MHz, DMSO-*d*₆) δ: 6.76 (d, *J* = 10.0 Hz, 1H, H3), 7.65–7.73 (m, 2H, H7 H8), 7.88 (dd, *J* = 7.7 and 1.3 Hz, 1H, H6), 8.25 (d, *J* = 10.0 Hz, 1H, H4), 12.3 (br s, 1H, NH). ¹³C NMR (100

MHz, DMSO- d_6) δ : 111.9 (C), 118.9 (CH), 121.5 (CH), 125.8 (CH), 130.6 (CH), 134.7 (CH), 140.7 (C), 146.7 (C), 161.3 (C).

8-nitroquinolin-2(1*H*)-one 20 (C₉H₆N₂O₃) was isolated and recrystallized in isopropanol to yield a yellow solid (96%, 10.6 mmol, 2.02 g), mp 163 °C (Lit: 163 °C), ¹H NMR (400 MHz, CDCl₃) δ : 6.79 (dd, *J* = 9.7 and 2.0 Hz, 1H, H3), 7.32–7.36 (m, 1H, H6), 7.82 (d, *J* = 9.7 and 1.4 Hz, 1H, H4), 7.91 (dd, *J* = 7.6 Hz, 1H, H5), 8.53 (dd, *J* = 8.4 and 1.4 Hz, 1H, H7), 11.3 (br s, 1H, NH). ¹³C NMR (100 MHz, DMSO- d_6) δ : 121.4 (CH), 122.1 (C), 123.8 (CH), 127.9 (CH), 133.1 (C), 133.9 (C), 135.6 (CH), 139.9 (CH), 161.6 (C).

Preparation of 4-bromomethyl-8-nitroquinolin-2(1*H*)-one 8

Carbon tetrachloride (15 mL) was added onto 400mg of 4-methyl-8-nitroquinolin-2(1*H*)-one (1.9 mmol, 1 equiv.) and 1.7 g of *N*-bromosuccinimide (9.7 mmol, 5 equiv.). The reaction mixture was heated at 80 °C. Then 31 mg of AIBN (0.24 mmol, 0.1 equiv.) were added, and stirred overnight. The reaction mixture was poured into water, extracted twice with dichloromethane and once with ethyl acetate. The combined organic layers were washed with water, dried over anhydrous MgSO₄ and evaporated *in vacuo*. The crude residue was purified by chromatography on silica gel using ethyl acetate as an eluent. 4-bromomethyl-8-nitroquinolin-2 (1*H*)-one 8 was isolated to yield a yellow solid (21%, 0.42 mmol, 120 mg).

Compound **8** (C₁₀H₇BrN₂O₃): mp 161 °C, ¹H NMR (400 MHz, CDCl₃) δ : 4.60 (s, 2H, CH₂), 6.87 (d, *J* = 2.0 Hz, 1H, H3), 7.40–7.44 (m, 1H, H6), 8.18 (dd, *J* = 1.3 and 8.8 Hz, 1H, H5), 8.57 (dd, *J* = 1.3 and 8.3 Hz, 1H, H7), 11.44 (br s, 1H, NH). ¹³C NMR (100 MHz, CDCl₃) δ : 27.9 (CH₂), 120.2 (C), 121.3 (CH), 123.7 (CH), 128.4 (CH), 132.4 (CH), 133.6 (C), 134.4 (C), 146.1 (C), 160.7 (C). HRMS (DCI CH₄) calcd for C₁₀H₈BrN₂O₃ [M+H]⁺ 282.9718, found 282.9723.

Preparation of 4-hydroxymethyl-8-nitroquinolin-2(1*H*)-one 9

Fifty milliliters of a mixture H₂O/THF (1/1) were added onto 150mg of 4-bromomethyl-8-nitroquinolin-2(1*H*)-one (0.53 mmol, 1 equiv). 106mg of NaOH (2.6 mmol, 5 equiv.) were added and the reaction mixture was stirred at 50 °C for 24 h. The reaction mixture was then poured into water, extracted twice with dichloromethane and twice with ethyl acetate. The combined organic layers were washed with water, dried over anhydrous MgSO₄ and evaporated *in vacuo*. The crude residue was purified by chromatography on silica gel using ethyl acetate as an eluent. 4-hydroxymethyl-8-nitroquinolin-2 (1*H*)-one 9 was isolated to yield a yellow solid (43%, 0.23 mmol, 50 mg).

Compound **9** (C₁₀H₈N₂O₄): mp 211 °C, ¹H NMR (300 MHz, DMSO) δ : 4.80 (d, *J* = 5.5 Hz, 2H, CH₂), 5.67 (t, *J* = 5.5 Hz, 1H, OH), 6.73 (s, 1H, H3), 7.37–7.42 (m, 1H, H6), 8.13 (d, *J* = 7.9 Hz, 1H, H5), 8.42 (d, *J* = 8.3 Hz, 1H, H7), 11.01 (br s, 1H, NH). ¹³C NMR (150 MHz, DMSO) δ : 39.5 (CH₂), 122.0 (CH), 122.1 (C), 123.0 (CH), 128.2 (CH), 133.3 (CH), 133.8 (CH), 136.5 (C), 141.3 (C), 161.6 (C). HRMS (DCI CH₄) calcd for C₁₀H₉N₂O₄ [M+H]⁺ 221.0562, found 221.0558.

Preparation of 4-[[2-(*N*-boc-2-aminoethoxy)ethoxy]ethyl] aminomethyl-8-nitroquinolin-2(1*H*)-one 10

THF (50 mL) was added onto 500 mg of 4-bromomethyl-8-nitroquinolin-2(1*H*)-one (1.8 mmol, 1 equiv.) and 1.3 g of *N*-Boc-2,2'-(ethylenedioxy)-diethylamine (5.3 mmol, 3 equiv.). Triethylamine (375 μ L, 2.7 mmol, 1.5 equiv.) were then added and the reaction mixture was stirred at 50 °C overnight. The reaction mixture was evaporated *in vacuo*. The crude product was then resolubilized in ethyl acetate, washed three times with water, dried over anhydrous MgSO₄ and evaporated *in vacuo*. The crude residue was purified by chromatography on silica gel using diethyl ether/methanol/20% aqueous ammonia solution (8.9/1/0.1) as an eluent. 4-[[2-(*N*-boc-2-aminoethoxy)ethoxy]ethyl] aminomethyl-8-nitroquinolin-2(1*H*)-one 10 was isolated to yield an orange oil (84%, 1.5 mmol, 680 mg).

Compound **10** (C₂₁H₃₀N₄O₇): ¹H NMR (600 MHz, DMSO) δ : 1.36 (s, 9H, *t*Bu), 2.5 (s, 1H, NH amine), 2.75–2.77 (m, 2H, CH₂ 3'), 3.03–3.06 (m, 2H, CH₂ 10'), 3.36–3.39 (m, 2H, CH₂ 4'), 3.51–3.54 (m, 6H, 3xCH₂ 6' 7' 9'), 4.02 (s, 2H, CH₂ 1'), 6.73 (br s, 1H, NH carbamate), 6.76 (s, 1H, H3), 7.38–7.42 (m, 1H, H6), 8.31 (dd, *J* = 8.1 and 1.3 Hz, 1H, H5), 8.42 (dd, *J* = 8.1 and 1.3 Hz, 1H, H7), 11.03 (br s, 1H, NH).

¹³C NMR (150 MHz, DMSO) δ : 28.7 (3 CH₃, *t*Bu), 40.1 (CH₂), 48.7 (CH₂), 49.9 (CH₂), 69.6 (CH₂), 70.0 (CH₂), 70.1 (CH₂), 70.5 (CH₂), 78.0 (C), 120.5 (CH), 121.4 (C), 121.6 (CH), 127.8 (CH), 132.9 (CH), 133.6 (C), 134.5 (C), 150.6 (C), 156.0 (C), 161.1 (C). HRMS (ESI) calcd for C₂₁H₃₁N₄O₇ [M+H]⁺ 450.2114, found 450.2118.

Preparation of 4-[[2-(2-aminoethoxy)ethoxy]ethyl]aminomethyl-8-nitroquinolin-2(1*H*)-one 11

Hydrochloric acid (15 mL of 5 N HCL in isopropanol) was added onto 600 mg of 4-[[2-(*N*-boc-2-aminoethoxy)ethoxy]ethyl] aminomethyl-8-nitroquinolin-2(1*H*)-one (1.33 mmol, 1 equiv.) and the reaction mixture was then stirred at rt for 4 h. The reaction mixture was successively poured into water, neutralized with K₂CO₃ and extracted several times with dichloromethane. The organic layer was dried over anhydrous Na₂SO₄ and evaporated *in vacuo*. 4-[[2-(2-aminoethoxy)ethoxy]ethyl] aminomethyl-8-nitroquinolin-2(1*H*)-one 11 was isolated to yield an oil in (43%, 0.57 mmol, 200 mg).

Compound **11** (C₁₆H₂₂N₄O₅): ¹H NMR (400 MHz, DMSO) δ : 2.5 (s, 1H, NH amine), 2.63–2.66 (m, 2H, CH₂ 10'), 2.74–2.77 (m, 2H, CH₂ 3'), 3.35–3.38 (m, 2H, CH₂ 9'), 3.49–3.55 (m, 6H, 3xCH₂ 4' 6' 7'), 4.01 (d, *J* = 1.9 Hz, 2H, CH₂ 1'), 6.76 (br s, 1H, H3), 7.38–7.42 (m, 1H, H6), 8.30 (dd, *J* = 8.1 and 1.3 Hz, 1H, H5), 8.40 (dd, *J* = 8.1 and 1.3 Hz, 1H, H7), 11.0 (br s, 1H, NH lactame). ¹³C NMR (150 MHz, DMSO) δ : 41.7 (CH₂), 48.7 (CH₂), 50.0 (CH₂), 70.0 (CH₂), 70.1 (CH₂), 70.6 (CH₂), 73.2 (CH₂), 120.4 (CH), 121.4 (C), 121.5 (CH), 127.7 (CH), 132.8 (CH), 133.7 (C), 134.6 (C), 150.7 (C), 161.2 (C). HRMS (ESI) calcd for C₁₆H₂₃N₄O₅ [M+H]⁺ 351.1668, found 351.1674.

Preparation of 4-bromo-8-nitroquinolin-2(1*H*)-one 13 [17]

Acetonitrile (10 mL) and 500 μ L of a 70% perchloric acid solution (5.4 mmol, 6 equiv.) were added onto 300 mg of 2,4-dibromo-8-nitroquinoline (0.90 mmol, 1 equiv.) in a sealed

tube. The reaction mixture was then heated at 100 °C in a microwave reactor during 1 h. The reaction mixture was poured into ice, neutralized with K₂CO₃ and extracted three times with dichloromethane. The organic layer was washed with water, dried over anhydrous Na₂SO₄ and evaporated *in vacuo*. 4-bromo-8-nitroquinolin-2(1*H*)-one **13** was isolated and recrystallized in acetonitrile to yield a yellow solid (87%, 0.78 mmol, 211 mg).

Compound **13** (C₉H₅BrN₂O₃): mp 239 °C (Lit: 240 °C), ¹H NMR (300 MHz, CDCl₃) δ: 7.20 (d, *J* = 2.0 Hz, 1H, H3), 7.37–7.42 (m, 1H, H6), 8.36 (dd, *J* = 8.0 and 1.4 Hz, 1H, H5), 8.58 (dd, *J* = 8.3 and 1.4 Hz, 1H, H7), 11.42 (br s, 1H, NH). ¹³C NMR (100 MHz, DMSO) δ: 121.0 (C), 122.6 (CH), 126.9 (CH), 129.4 (CH), 132.7 (C), 134.8 (C), 135.5 (CH), 136.5 (C), 159.5 (C).

Preparation of *N*-methylquinolin-2(1*H*)-one **16** [36]

DMF (30 mL) was added onto 1 g of quinoline-2(1*H*)-one (6.9 mmol, 1 equiv.), 1.43 g of K₂CO₃ (10.3 mmol, 1.5 equiv.). The reaction mixture was heated at 80 °C and 430 μL of methane iodide (6.9 mmol, 1 equiv.) were added dropwise. After 48 h, the reaction mixture was poured into water and extracted three times with dichloromethane. The organic layer was washed 5 times with water, dried over anhydrous Na₂SO₄ and evaporated *in vacuo*. The crude residue was purified by chromatography on silica gel using dichloromethane/ethyl acetate (7.5/2.5) as eluent. *N*-methylquinolin-2(1*H*)-one **16** was isolated and recrystallized in isopropanol to yield a white solid (71%, 4.90 mmol, 780 mg).

Compound **16** (C₁₀H₉NO): mp 76 °C (Lit: 74 °C), ¹H NMR (400 MHz, CDCl₃) δ: 3.73 (s, 3H, CH₃), 6.71 (d, *J* = 9.4 Hz, 1H, H3), 7.21–7.25 (m, 1H, H6), 7.37 (dd, *J* = 8.1 and 1.0 Hz, 1H, H5), 7.55–7.59 (m, 2H, H7 - H8), 7.67 (d, *J* = 9.5 Hz, 1H, H4). ¹³C NMR (100 MHz, CDCl₃) δ: 29.4 (CH₃), 114.1 (CH), 120.6 (C), 121.7 (CH), 122.1 (CH), 128.7 (CH), 130.6 (CH), 138.9 (CH), 140.0 (C), 162.3 (C).

Preparation of 2-methoxy-8-nitroquinoline **21** [16]

Under Argon atmosphere, 100mg of 8-nitroquinolin-2(1*H*)-one (0.53 mmol, 1 equiv.) were solubilized in 5mL of DMF and were added onto a DMF solution (5 mL) of 42 mg of 60% sodium hydride (1.05 mmol, 2 equiv.). After 10 min of stirring at rt, 65 μL of methyl iodide (1.05 mmol, 2 equiv.) were added dropwise. After one night stirring at rt, the reaction mixture was poured into ice. The resulting precipitate was filtered and dried *in vacuo*. The crude residue was purified by chromatography on silica gel using diethyl ether as eluent. 2-methoxy-8-nitroquinoline **21** was isolated and recrystallized in cyclohexane to yield a pale white solid (64%, 0.34 mmol, 70 mg).

Compound **21** (C₁₀H₈N₂O₃): mp 125 °C (Lit: 114 °C), ¹H NMR (400 MHz, CDCl₃) δ: 4.09 (s, 3H, CH₃), 7.05 (d, *J* = 8.9 Hz, 1H, H3), 7.42–7.46 (m, 1H, H6), 7.93 (dd, *J* = 8.1 and 1.4 Hz, 1H, H5), 7.99 (dd, *J* = 7.6 and 1.4 Hz, 1H, H7), 8.07 (d, *J* = 8.9 Hz, 1H, H4). ¹³C NMR (100 MHz, CDCl₃) δ: 54.1 (CH₃), 115.1 (CH), 122.6 (CH), 124.0 (CH), 126.2 (C), 131.5 (CH), 138.2 (C), 138.5 (CH), 146.6 (C), 163.7 (C).

Preparation of 3-bromo-8-nitroquinolin-2(1H)-one **22**

Fifty milliliters of a 48% hydrobromic acid solution were added onto 1.34 g of 8-nitroquinolin-2(1H)-one (7.05 mmol, 1 equiv.). The reaction mixture was then stirred at 100 °C. Then 3.2 g of sodium bromate (21.1 mmol, 3 equiv.) were added with precaution (Br₂ formation). After 5 h under reflux, the reaction mixture was left for 2 h under the hood to evacuate remaining Br₂ vapors, and then poured into ice, neutralized with K₂CO₃ and extracted three times with dichloromethane. The organic layer was washed with water, dried over anhydrous Na₂SO₄ and evaporated *in vacuo*.

The crude residue was purified by chromatography on silica gel using cyclohexane/ethyl acetate (1/1) as an eluent. 3-bromo-8-nitroquinolin-2(1H)-one **22** was isolated and recrystallized in acetonitrile to yield a yellow solid (68%, 4.8 mmol, 1.3 g).

Compound **22** (C₉H₅BrN₂O₃): mp 216 °C, ¹H NMR (400 MHz, CDCl₃) δ: 7.36–7.40 (m, 1H, H6), 7.89 (dd, *J* = 8.4 and 1.4 Hz, 1H, H5), 8.6 (s, 1H, H4), 8.56 (dd, *J* = 7.7 and 1.6 Hz, 1H, H7), 11.51 (br s, 1H, NH). ¹³C NMR (100 MHz, CDCl₃) δ: 119.9 (C), 122.1 (CH), 122.3 (C), 128.0 (CH), 132.9 (C), 133.2 (C), 134.8 (CH), 141.0 (CH), 157.5 (C). HRMS (DCI CH₄) calcd for C₉H₆BrN₂O₃ [M+H]⁺ 268.9562, found 268.9554.

Preparation of 3-chloro-8-nitroquinolin-2(1H)-one **23**

Fifty milliliters of a 37% hydrochloric acid solution were added onto 1 g of 8-nitroquinolin-2(1H)-one (5.3 mmol, 1 equiv.). The reaction mixture was then stirred at 100 °C before 1.7 g of sodium chlorate (15.8 mmol, 3 equiv.) were added with precaution (Cl₂ formation). After 45 min under reflux, the reaction mixture was left for 2 h under the hood to evacuate remaining Cl₂ vapors, and then was poured into ice, neutralized with K₂CO₃ and extracted three times with dichloromethane. The organic layer was washed with water, dried over anhydrous Na₂SO₄ and evaporated *in vacuo*. The crude residue was purified by chromatography on silica gel using diethyl ether as an eluent. 3-chloro-8-nitroquinolin-2(1H)-one **23** was isolated and recrystallized in acetonitrile to yield a yellow solid (62%, 3.3 mmol, 738 mg).

Compound **23** (C₉H₅ClN₂O₃): mp 195 °C, ¹H NMR (400 MHz, CDCl₃) δ: 7.37–7.41 (m, 1H, H6), 7.88 (dd, *J* = 7.7 and 1.4 Hz, 1H, H5), 8.04 (s, 1H, H4), 8.55 (dd, *J* = 8.4 and 1.4 Hz, 1H, H7), 11.56 (br s, 1H, NH). ¹³C NMR (100 MHz, CDCl₃) δ: 121.8 (C), 122.2 (CH), 127.9 (CH), 129.2 (C), 132.3 (C), 133.1 (C), 134.9 (CH), 137.0 (CH), 157.5 (C). HRMS (DCI CH₄) calcd for C₉H₆ClN₂O₃ [M+H]⁺ 225.0067, found 225.0070.

Preparation of 3-bromo-2-methoxy-8-nitroquinoline **24**

Under Argon atmosphere, 250 mg of 3-bromo-8-nitroquinolin-2(1H)-one (0.93 mmol, 1 equiv.) were solubilized in 5 mL of dry DMF and were added onto a DMF solution (5 mL) of 74 mg of 60% sodium hydride (1.86 mmol, 2 equiv.). After 10 min of stirring at rt, 115 μL of methyl iodide (1.86 mmol, 2 equiv.) were added dropwise. The reaction mixture was stirred at rt overnight, before being poured into ice. The resulting precipitate was filtered and dried *in vacuo*. The crude residue was purified by chromatography on silica gel using

cyclohexane/acetone (9/1) as eluent. 3-bromo-2-methoxy-8-nitroquinoline **24** was isolated to yield a pale white solid (55%, 0.51 mmol, 146 mg).

Compound **24** (C₁₀H₇BrN₂O₃): mp 208 °C, ¹H NMR (300 MHz, CDCl₃) δ: 4.15 (s, 3H, CH₃), 7.43–7.49 (m, 1H, H6), 7.86 (dd, *J* = 8.1 and 1.4 Hz, 1H, H5), 8.02 (dd, *J* = 7.7 and 1.4 Hz, 1H, H7), 8.35 (s, 1H, H4). ¹³C NMR (100 MHz, CDCl₃) δ: 55.4 (CH₃), 110.4 (C), 123.5 (CH), 124.4 (CH), 127.1 (C), 130.6 (CH), 136.7 (C), 140.6 (CH), 146.2 (C), 159.2 (C). HRMS (DCI CH₄) calcd for C₁₀H₇BrN₂O₃ [M+H]⁺ 282.9718, found 282.9722.

Preparation of 8-amino-3-bromoquinolin-2(1*H*)-one **25**

Ethanol (20 mL) was added onto 300 mg of 3-bromo-8-nitroquinolin-2(1*H*)-one (1.11 mmol, 1 equiv.) and 1.1 g of tin (II) chloride (5.55 mmol, 5 equiv.). The reaction mixture was refluxed for 3 h. The reaction mixture was then neutralized into an aqueous solution of Na₂CO₃, filtered on celite, extracted three times with dichloromethane and once with ethyl acetate. The combined organic layers were washed with water, dried over anhydrous Na₂SO₄ and evaporated *in vacuo*. The crude residue was purified by chromatography on silica gel using dichloromethane/methanol (95/5) as eluent. 8-amino-3-bromoquinolin-2(1*H*)-one **25** was isolated to yield a pale brown solid (53%, 0.59 mmol, 140 mg).

Compound **25** (C₉H₇BrN₂O): Dec. 248 °C, ¹H NMR (400 MHz, DMSO-*d*₆) δ: 5.60 (br s, 2H, NH₂), 6.84 (dd, *J* = 7.5 and 1.5 Hz, 1H, H7), 6.90 (dd, *J* = 7.7 and 1.5 Hz, 1H, H5), 6.95–6.99 (m, 1H, H6), 8.40 (s, 1H, H4), 11.35 (br s, 1H, NH). ¹³C NMR (100 MHz, DMSO-*d*₆) δ: 115.2 (CH), 115.5 (CH), 116.6 (C), 120.6 (C), 123.5 (CH), 125.6 (C), 135.4 (C), 143.2 (CH), 158.3 (C). HRMS (DCI CH₄) calcd for C₉H₇BrN₂O₃ [M+H]⁺ 238.9820, found 238.9820.

General procedure for the preparation of 5-methyl-8-nitroquinolin-2(1*H*)-one **26**, 6-methyl-8-nitroquinolin-2(1*H*)-one **27** [37], 7-methyl-8-nitroquinolin-2(1*H*)-one **28**, 5-methoxy-8-nitroquinolin-2(1*H*)-one **29**, 6-methoxy-8-nitroquinolin-2(1*H*)-one **30** [38] and 7-methoxy-8-nitroquinolin-2(1*H*)-one **31**.

In a first step, according to a previously reported procedure [21], 1.2 equiv. of 3,3'-diethoxyacryloyl chloride (prepared from ethyl 3,3'-diethoxypropionate by successive saponification and reaction with SOCl₂) was reacted at rt with 1 equiv. of the appropriate nitroaniline derivative in dichloromethane, in the presence of 2 equiv. of pyridine. The reaction mixtures were then poured into water and extracted three times with dichloromethane. The organic layers were washed with brine, dried over anhydrous Na₂SO₄ and evaporated *in vacuo*. In a second step, each crude residue was reacted with 98% sulfuric acid and stirred at rt for 3–4 h (monitored by TLC). The reaction mixtures were then poured into ice, neutralized with K₂CO₃ and extracted three times with dichloromethane. The organic layers were washed with water, dried over anhydrous Na₂SO₄ and evaporated *in vacuo*. The final crude residues were purified by chromatography on silica gel.

5-methyl-8-nitroquinolin-2(1*H*)-one **26** (C₁₀H₈N₂O₃) was purified by chromatography on silica gel using cyclohexane/ethyl acetate (90/10) as eluent, isolated and recrystallized in acetonitrile to yield a pale brown solid (46%, 2.39 mmol, 490 mg), mp 213 °C, ¹H NMR

(400 MHz, DMSO- d_6) δ : 2.67 (s, 3H, CH₃), 6.78 (dd, J = 10.0 and 2.2 Hz, 1H, H3), 7.15 (dd, J = 8.5 and 0.6 Hz, 1H, H6), 7.99 (d, J = 10.0 Hz, 1H, H4), 8.40 (d, J = 8.5 Hz, 1H, H7), 11.5 (br s, 1H, NH). ¹³C NMR (100 MHz, DMSO- d_6) δ : 19.8 (CH₃), 120.1 (C), 123.1 (CH), 123.3 (CH), 127.8 (CH), 131.7 (C), 134.1 (C) 136.6 (CH), 145.4 (C), 161.3 (C). HRMS (DCI CH₄) calcd for C₁₀H₉N₂O₃ [M+H]⁺ 205.0613, found 205.0608.

6-methyl-8-nitroquinolin-2(1*H*)-one 27 (C₁₀H₈N₂O₃) was purified by chromatography on silica gel using cyclohexane/ethyl acetate (90/10) as eluent and isolated to yield a brown solid (6%, 0.34 mmol, 70 mg), mp 200 °C (Lit: 199–200), ¹H NMR (400 MHz, CDCl₃) δ : 2.50 (s, 3H, CH₃), 6.74 (dd, J = 9.7 and 2.0 Hz, 1H, H3), 7.69 (s, 1H, H5), 7.74 (d, J = 9.7 Hz, 1H, H4), 8.33 (d, J = 2.0 Hz, 1H, H7), 11.22 (br s, 1H, NH). ¹³C NMR (100 MHz, CDCl₃) δ : 20.5 (CH₃), 122.0 (C), 123.7 (CH), 128.4 (CH), 131.7 (C), 131.8 (C), 132.8 (C), 135.9 (CH) 139.7 (CH), 161.6 (C).

7-methyl-8-nitroquinolin-2(1*H*)-one 28 (C₁₀H₈N₂O₃) was purified by chromatography on silica gel using cyclohexane/ethyl acetate (90/10) as eluent, isolated and recrystallized in acetonitrile to yield a yellow solid (52%, 3.42 mmol, 700 mg), mp 233 °C, ¹H NMR (400 MHz, CDCl₃) δ : 2.64 (s, 3H, CH₃), 6.69 (d, J = 9.6 Hz, 1H, H6), 7.15 (dd, J = 8.0 and 0.6 Hz, 1H, H3), 7.64 (d, J = 8.0 Hz, 1H, H4), 7.74 (d, J = 9.6 Hz, 1H, H5), 10.12 (br s, 1H, NH). ¹³C NMR (100 MHz, CDCl₃) δ : 21.2 (CH₃), 119.7 (C), 122.7 (CH), 125.5 (CH), 132.2 (CH), 132.6 (C), 135.6 (C) 137.6 (C), 139.9 (CH), 161.7 (C). HRMS (DCI CH₄) calcd for C₁₀H₉N₂O₃ [M+H]⁺ 205.0613, found 205.0615.

5-methoxy-8-nitroquinolin-2(1*H*)-one 29 (C₁₀H₈N₂O₄) was purified by chromatography on silica gel using cyclohexane/ethyl acetate (90/10) as eluent, isolated and recrystallized in acetonitrile to yield a dark orange solid (21%, 0.61 mmol, 135 mg), mp 246 °C, ¹H NMR (400 MHz, CDCl₃) δ : 4.09 (s, 3H, OCH₃), 6.68 (dd, J = 10.0 and 2.1 Hz, 1H, H3), 6.73 (d, J = 9.4 Hz, 1H, H6), 8.17 (d, J = 9.9 Hz, 1H, H4), 8.52 (d, J = 9.4 Hz, 1H, H7), 11.45 (br s, 1H, NH). ¹³C NMR (100 MHz, CDCl₃) δ : 56.8 (OCH₃), 102.8 (CH), 110.7 (C), 121.8 (CH), 127.0 (C), 130.6 (CH), 134.6 (CH) 135.6 (C), 161.7 (C), 161.8 (C). HRMS (DCI CH₄) calcd for C₁₀H₉N₂O₃ [M+H]⁺ 221.0562, found 221.0561.

6-methoxy-8-nitroquinolin-2(1*H*)-one 30 (C₁₀H₈N₂O₄) was purified by chromatography on silica gel using cyclohexane/ethyl acetate (90/10) as eluent and isolated to yield a pale brown solid (4%, 0.05 mmol, 12 mg), mp 210 °C (Lit: 210–211 °C), ¹H NMR (400 MHz, CDCl₃) δ : 3.93 (s, 3H, OCH₃), 6.76 (dd, J = 9.7 and 1.8 Hz, 1H, H3), 7.42 (d, J = 2.9 Hz, 1H, H5), 7.73 (d, J = 9.7 Hz, 1H, H4), 8.07 (d, J = 2.9 Hz, 1H, H7), 11.15 (br s, 1H, NH). ¹³C NMR (100 MHz, CDCl₃) δ : 56.3 (OCH₃), 113.5 (CH), 113.9 (C), 120.7 (CH), 122.9 (C), 124.4 (CH), 128.3 (C) 139.4 (CH), 153.5 (C), 161.4 (C).

7-methoxy-8-nitroquinolin-2(1*H*)-one 31 (C₁₀H₈N₂O₄) was purified by chromatography on silica gel using dichloromethane/ethyl acetate (90/10) as eluent, isolated and recrystallized in acetonitrile to yield a yellow solid (45%, 0.79 mmol, 175 mg), mp 244 °C, ¹H NMR (400 MHz, CDCl₃) δ : 4.04 (s, 3H, OCH₃), 6.57 (d, J = 9.6 Hz, 1H, H3), 6.93 (d, J = 8.9 Hz, 1H, H6), 7.68 (d, J = 9.3 Hz, 2H, H4 H5), 9.9 (br s, 1H, NH). ¹³C NMR (100 MHz, CDCl₃) δ : 57.2 (OCH₃), 105.0 (C), 106.9 (CH), 114.3 (C), 120.6 (CH), 133.5 (CH), 133.7 (C) 139.9

(CH), 155.9 (C), 161.8 (C). HRMS (DCI CH₄) calcd for C₁₀H₉N₂O₃ [M+H]⁺ 221.0562, found 221.0556.

Electrochemistry

Voltammetric measurements were carried out with a potentiostat Autolab PGSTAT100 (ECO Chemie, The Netherlands) controlled by GPES 4.09 software. Experiments were performed at room temperature in a homemade airtight three-electrode cell connected to a vacuum/argon line. The reference electrode consisted of a saturated calomel electrode (SCE) separated from the solution by a bridge compartment. The counter electrode was a platinum wire of approximately 1 cm [2] apparent surface. The working electrode was GC microdisk (1.0 mm of diameter – Biologic SAS). The supporting electrolyte (nBu₄N)[PF₆] (Fluka, 99% puriss electrochemical grade) and the solvent DMSO (Sigma-Aldrich puriss p. a. dried <0.02% water) were used as received and simply degassed under argon. The solutions used during the electrochemical studies were typically 10⁻³ M in compound and 0.1 M in supporting electrolyte. Before each measurement, the solutions were degassed by bubbling Ar and the working electrode was polished with a polishing machine (Presi P230). Under these experimental conditions employed in this work, the half-wave potential (E_{1/2}) of the ferrocene Fc⁺/Fc couple in DMSO was E_{1/2} = 0.45 V vs SCE. Experimental peak potentials have been measured versus SCE and converted to NHE by adding 0.241 V.

Computational studies

All the calculations were carried out with the GAUSSIAN 09 suite [39]. Geometry optimizations were performed with the M06-2x [40] density functional and the 6-311++G (2 d, 2p) basis set. Previous studies have indicated that extended basis sets, with diffuse s- and p-type functions and polarization functions were important for the description of the electronic affinity of nitrobenzene derivatives [22,23]. The effect of solvation were described with the self-consistent reaction field (SCRF) method using the integral equation formalism polarizable continuum Model (IEFPCM) with DMSO as solvent [41]. Vibrational frequency calculation were used to confirm the convergence to local minima and to calculate the unscaled zero-point-energy (ZPE) and the entropy corrections at 298 K. The standard variation of the Gibb's free energies were calculated as the energy difference between anionradical and neutral forms after full geometry optimization according to the following equation: R-NO₂ + 1 e⁻ → . R - NO₂⁻. Reduction potentials of the nitro-compounds were calculated using the equation based on Faraday's law:

$$E^{\circ} = -\frac{\Delta G_{red}}{nF} + E_H^0 \quad (1)$$

where G_{red} is the Gibbs free energy of reduction, n is the number of electrons transferred (i.e. one electron), F is the Faraday constant which equals 23.06 kcal mol⁻¹. V⁻¹ and E_H^0 is the absolute potential of the normal hydrogen electrode. The E_H^0 value was taken as -4.28 V [42].

Biology

Antileishmanial activity on *L. infantum* axenic amastigotes. [43]

L. infantum promastigotes (MHOM/MA/67/ITMAP-263, CNR Leishmania, Montpellier, France, expressing luciferase activity) in logarithmic phase cultivated in RPMI 1640 medium supplemented with 5% foetal calf serum (FCS), 2 mM L-glutamine and antibiotics (100 U/mL penicillin and 100 µg/mL streptomycin), were centrifuged at 900 g for 10 min. The supernatant was removed carefully and was replaced by the same volume of RPMI 1640 complete medium at pH 5.4 and incubated for 24 h at 24 °C. The acidified promastigotes were incubated for 24 h at 37 °C in a ventilated flask. Promastigotes were then transformed into axenic amastigotes. The effects of the tested compounds on the growth of *L. infantum* axenic amastigotes were assessed as follows. *L. infantum* amastigotes were incubated at a density of 2.10⁶ parasites/mL in sterile 96-well plates with various concentrations of compounds dissolved in DMSO (final concentration less than 0.5% v/v), in duplicate. Appropriate controls DMSO, amphotericin B, miltefosine and fexinidazole (reference drugs purchased from Sigma Aldrich) were added to each set of experiments. After a 48 h incubation period at 37 °C, each plate-well was then microscope-examined for detecting any precipitate formation. To estimate the luciferase activity of axenic amastigotes, 80 µL of each well are transferred to white 96-well plates, Steady Glow[®] reagent (Promega) was added according to manufacturer's instructions, and plates were incubated for 2 min. The luminescence was measured in Microbeta Luminescence Counter (PerkinElmer). Inhibitory concentration 50% (IC₅₀) was defined as the concentration of drug required to inhibit by 50% the metabolic activity of *L. infantum* amastigotes compared to control. IC₅₀ values were calculated by non-linear regression analysis processed on dose response curves, using TableCurve 2D V5 software. IC₅₀ values represent the mean of three independent experiments.

Antileishmanial activity on *L. donovani* promastigotes

The effects of the tested compounds on the growth of *L. donovani* promastigotes (MHOM/IN/00/DEVI) were assessed by MTT assay [44]. Briefly, promastigotes in logarithmic phase in Schneider's medium supplemented with 20% foetal calf serum (FCS), 2 mM L-glutamine and antibiotics (100 U/mL penicillin and 100 µg/mL streptomycin), were incubated at an average density of 10⁶ parasites/mL in sterile 96-well plates with various concentrations of compounds dissolved in DMSO (final concentration less than 0.5% v/v), in duplicate. Appropriate controls treated by DMSO, miltefosine or amphotericin B (reference drugs purchased from Sigma Aldrich) were added to each set of experiments. After a 72 h incubation period at 27 °C, parasite metabolic activity was determined. Each plate-well was then microscope-examined for detecting possible precipitate formation. 10 µL of MTT (3-(4,5-dimethylthiazol-2-yl)-2,5-diphenyltetrazolium bromide) solution (10 mg/mL in PBS) were added to each well followed by incubation for another 4 h. The enzyme reaction was then stopped by addition of 100 µL of 50% isopropanol–10% sodium dodecyl sulfate. Plates were shaken vigorously (300 rpm) for 10 min. The absorbance was finally measured at 570nm in a BIO-TEK ELx808 Absorbance Microplate Reader. Inhibitory concentration 50% (IC₅₀) was defined as the concentration of drug required to inhibit by 50% the metabolic activity of *L. donovani* and promastigotes compared to the

control. IC₅₀ were calculated by nonlinear regression analysis processed on dose–response curves, using TableCurve 2D V5.0 soft ware. IC₅₀ values represent the mean value calculated from three independent experiments.

Antileishmanial activity on *L. donovani* intracellular amastigotes

The effects of the tested compounds on the growth of *Leishmania donovani* intracellular amastigotes (MHOM/IN/00/DEVI) were assessed according to the method of Da Luz et al. [45] 400 µL of THP-1 cells activated with Phorbol 12-Myristate 13-Acetate (final concentration: 50 ng/mL) were seeded in sterile chamber-slides at an average density of 10⁵ cells/mL and incubated for 48 h at 37 °C and 6% CO₂. *L. donovani* promastigotes were centrifuged at 900 g for 10 min and the supernatant replaced by the same volume of Schneider 20% FCS pH 5.4 and incubated for 24 h at 27 °C. THP-1 cells were then infected by acidified promastigotes at an average density of 10⁶ cells/mL (10:1 ratio) and chamber-slides incubated for 24 h at 37 °C. Then, in duplicate, the medium containing various concentrations of tested-compounds was added (final DMSO concentration being inferior to 0.5% v/v). Appropriate controls treated with or without solvent (DMSO), and various concentrations of miltefosine and amphotericin B (reference drugs purchased from Sigma Aldrich) were added to each set of experiments. After 120 h incubation at 37 °C and 6% CO₂, well supernatant was removed. Cells were fixed with analytical grade methanol and stained with 10% Giemsa. The percentage of infected macrophages in each assay was determined microscopically by counting at least 200 cells in each sample. IC₅₀ was defined as the concentration of drug necessary to produce a 50% decrease of infected macrophages compared to the control. IC₅₀ were calculated by non-linear regression analysis processed on dose–response curves, using TableCurve 2D V5.0 software. IC₅₀ values represent the mean value calculated from three independent experiments.

Antileishmanial activity on *L. donovani* promastigotes NTR1 and NTR2 over-expressing strain

Cell lines and culture conditions: The clonal *Leishmania donovani* cell line LdBOB (derived from MHOM/SD/62/1 S-CL2D) was grown as promastigotes at 26 °C in modified M199 media, as previously described [46]. LdBOB promastigotes overexpressing NTR1 (LinJ.05.0660) [47] and NTR2 (LinJ.12.0730) [48] were grown in the presence of nourseothricin (100 µg ml⁻¹). *In vitro* drug sensitivity assays: To examine the effects of test compounds on growth, triplicate promastigote cultures were seeded with 5 × 10⁴ parasites ml⁻¹. Parasites were grown in 10 mL cultures in the presence of drug for 72 h, after which 200 µL aliquots of each culture were added to 96-well plates, 50 µM resazurin was added to each well and fluorescence (excitation of 528 nm and emission of 590 nm) measured after a further 4 h incubation [49]. Data were processed using GRAFIT (version 5.0.4; Erithacus software) and fitted to a 2-parameter equation, where the data are corrected for background fluorescence, to obtain the effective concentration inhibiting growth by 50%

$$(EC_{50}): y = \frac{100}{1 + \left(\frac{[I]}{EC_{50}}\right)^m}$$

In this equation [I] represents inhibitor concentration and m is the

slope factor. Experiments were repeated at least two times and the data is presented as the mean plus standard deviation.

Antitrypanosomal activity on *T. brucei brucei* trypomastigotes

Assays were performed on *Trypanosoma brucei brucei* AnTat 1.9 strain (IMTA, Antwerpen, Belgium). It was cultured in MEM with Earle's salts, supplemented according to the protocol of Baltz et al. [50] with the following modifications, 0.5 mM mercaptoethanol (Sigma Aldrich[®], France), 1.5 mM L-cysteine (Sigma Aldrich[®]), 0.05 mM bathocuproine sulfate (Sigma Aldrich[®]) and 20% heat-inactivated horse serum (Gibco[®], France), at 37 °C in an atmosphere of 5% CO₂. The parasites were incubated at an average density of 2000 parasites/well in sterile 96-wells plates (Mc2[®], France) with various concentrations of compounds dissolved in DMSO (Sigma Aldrich[®]), in duplicate. Reference drugs suramin, pentamidine, eflornithine, and fexinidazole (purchased from Sigma Aldrich, France and Fluorochem, UK) suspended in NaCl 0.9% or DMSO, were added to each set of experiments. The effects of the tested compounds were assessed by the viability marker Alamar Blue[®] (Fisher, France) assay described by R  z et al. [51] After a 69 h incubation period at 37 °C, 10 µL of Alamar Blue[®] was then added to each well, and the plates were incubated for 5 h [52]. The plates were read in a PerkinElmer ENSPIRE (Germany) microplate reader using an excitation wavelength of 530 nm and an emission wavelength of 590 nm. IC₅₀ were calculated by nonlinear regression analysis processed on dose-response curves, using GraphPad Prism software (USA). IC₅₀ was defined as the concentration of drug necessary to inhibit by 50% the viability of *T. brucei brucei* compared to the control. IC₅₀ values were calculated from three independent experiments in duplicate.

Antitrypanosomal activity on *T. b. brucei* trypomastigotes NTR1 over-expressing strain

Trypanosoma brucei bloodstream-form 'single marker' S427 (T7RPOL TETR NEO) and drug-resistant cell lines were cultured at 37 °C in HMI9-T medium [53] supplemented with 2.5 µg.mL⁻¹ G418 to maintain expression of T7 RNA polymerase and the tetracycline repressor protein. Bloodstream trypanosomes overexpressing the *T. brucei* nitroreductase (NTR1) [54] were grown in medium supplemented with 2.5 µg.mL⁻¹ phleomycin and expression of NTR was induced by the addition of 1 µg.mL⁻¹ tetracycline. Cultures were initiated with 1 × 10⁵ cells.mL⁻¹ and sub-cultured when cell densities approached 1–2 (× 10⁶). mL⁻¹.

In order to examine the effects of inhibitors on the growth of these parasites, triplicate cultures containing the inhibitor were seeded at 1 × 10⁵ trypanosomes.mL⁻¹. Cells overexpressing NTR were induced with tetracycline 48 h prior to EC₅₀ analysis. Cell densities were determined after culture for 72 h, as previously described [55]. EC₅₀ values were determined using the following two-parameter equation by non-linear regression using GraFit:

$$y = \frac{100}{1 + \left(\frac{[I]}{EC_{50}}\right)^m}$$

where the experimental data were corrected for background cell density and expressed as a percentage of the uninhibited control cell density. In this equation [I] represents inhibitor concentration and m is the slope factor.

Cytotoxic evaluation on HepG2 cell line

The evaluation of the tested molecules cytotoxicity on the HepG2 (hepatocarcinoma cell line from ECACC purchased from Sigma-Aldrich, ref 85011430-1 V L certificated without mycoplasma) was done according to the method of Mosman with slight modifications [44]. Briefly, cells (5×10^4 cells/mL) in 100 μ L of complete medium, [Alpha MEM Eagle from PAN BIOTECH supplemented with 10% foetal bovine serum, 2 mM L-glutamine and antibiotics (100 U/mL penicillin and 100 μ g/mL streptomycin)] were seeded into each well of 96-well plates and incubated at 37 °C and 5% CO₂. After a 24 h incubation, 100 μ L of medium with various product concentrations and appropriate controls were added and the plates were incubated for 72 h at 37 °C and 5% CO₂. Each plate-well was then microscope-examined for detecting possible precipitate formation before the medium was aspirated from the wells. 100 μ L of MTT solution (0.5 mg/mL in Alpha MEM Eagle) were then added to each well. Cells were incubated for 2 h at 37 °C and 5% CO₂. After this time, the MTT solution was removed and DMSO (100 μ L) was added to dissolve the resulting formazan crystals. Plates were shaken vigorously (300 rpm) for 5 min. The absorbance was measured at 570 nm with a microplate spectrophotometer (Eon BioTek). DMSO was used as blank and doxorubicin (purchased from Sigma Aldrich) as positive control. CC₅₀ were calculated by non-linear regression analysis processed on dose–response curves, using TableCurve 2D V5 software. CC₅₀ values represent the mean value calculated from three independent experiments.

Cytotoxic evaluation on THP1 cell line

The evaluation of the tested molecules cytotoxicity on the differentiated THP-1 cell line (acute monocytic leukemia cell line purchased from ATCC, ref TIB-202) was performed according to the method of Mosman with slight modifications [44]. Briefly, cells in 100 μ L of complete RPMI medium with Phorbol 12-Myristate 13-Acetate (final concentration: 50 ng/mL) were incubated at an average density of 10⁶ cells/mL and in sterile 96-well plates. After 48 h incubation, 100 μ L of medium with various product concentrations dissolved in DMSO (final concentration less than 0.5% v/v) were added and the plates were incubated for 72 h at 37 °C. Each plate-well was then microscope-examined for detecting possible precipitate formation before the medium was aspirated from the wells. 100 μ L of MTT solution (0.5 mg/mL in medium without FCS) were then added to each well. Cells were incubated for 2 h at 37 °C. After this time, the MTT solution was removed and DMSO (100 μ L) was added to dissolve the resulting blue formazan crystals. Plates were shaken vigorously (300 rpm) for 10 min. The absorbance was measured at 570 nm with 630 nm as reference wavelength spectrophotometer using a BIO-TEK ELx808 Absorbance Microplate Reader. DMSO was used as blank and doxorubicin (purchased from Sigma Aldrich) as positive control. Cell viability was calculated as percentage of control (cells incubated without compound). The 50% cytotoxic concentration was determined from the dose–response curve by using the TableCurve 2D V5.0 software.

Ames test method

Mutagenicity test was carried out by using a modified version [56] of the liquid incubation assay of the classical Ames test. *S. typhimurium* tester strains (TA97a, TA98, TA100 and

TA102) were grown overnight in a Nutrient Broth n°2 (Oxoid, France). After this period, 5–50 mM DMSO solutions of the tested drugs were added to 0.1 mL of culture and incubated with 4% S9 mix for 1 h at 37 °C with shaking. Each sample was assayed in duplicate. After incubation, 2 mL of molten top agar were mixed gently with the preincubated solution and poured onto Vogel-Bonner minimal agar plates. After 48 h at 37 °C in the dark, the number of spontaneous and drug induced revertants per plate was determined for each dose with a laser bacterial colony counter. A product was considered mutagenic when it induces a two-fold increase of the number of revertants, compared with the spontaneous frequency (negative control). Benzo [a]pyrene was used as a positive control with all *Salmonella* strains in presence of S9 mix.

Comet assay

The alkaline comet assay was used to detect DNA strand breaks and alkali-labile sites. Trypsinized HepG2 cells were embedded in 0.7% low-melting point agarose (Sigma “Low Gelling Temperature”) and laid on pre-cut sheets of polyester film (Gelbond® film) to perform minigel deposits as previously described [57]. Film were then placed in lysis solution (NaCl 2.5 M, Na₂EDTA 0.1 M, Tris 10 mM, 1% Triton X-100, 10% DMSO pH 10) for 18 h at 4 °C. Electrophoresis (with a solution which contained 0.3 M NaOH, 1 mM Na₂EDTA, pH > 13) was processed for 24 min in a tank with a power supply giving 28 V (resulting in 0.8 V/cm). After electrophoresis, films were immersed 2 × 5 min in PBS for neutralization, followed by fixation in 100% ethanol for 1.5 h and drying. After staining with SYBR® Gold (Life Technologies) at 10 000 X dilution for 20 min, films were observed at 20× magnification with an epifluorescence microscope equipped with an automated platform (Nikon NiE) and coupled to a camera (DS-Q1Mc) and the software Nikon NiS Element Advanced Research to automatically capture images. In these images, for each cell, the level of DNA damage was evaluated using a semi-automated scoring system, by measurement of the intensity of all tail pixels divided by the total intensity of all pixels in head and tail of comet, by means of the software “Lucia comet assay” (Laboratory Imaging, Prague Czech Republic). Fifty cells per deposit and four deposits per sample were analysed. The median from these 200 values was calculated, and named “% tail DNA”.

Microsomal stability and plasma protein binding assays

Microsomal stability assay—The tested product and propranolol, used as reference, are incubated in duplicate (reaction volume of 0.5 mL) with female mouse microsomes (CD-1, 20 mg/mL, BD Gentest™) at 37 °C in a 50 mM phosphate buffer, pH 7.4, in the presence of MgCl₂ (5 mM), NADP (1 mM), glucose-6-phosphate dehydrogenase (0.4 U/mL) and glucose-6-phosphate (5 mM). For the estimation of the intrinsic clearance: 50 µL aliquot at 0, 5, 10, 20, 30 and 40 min are collected and the reaction is stopped with 4 vol of acetonitrile (ACN) containing the internal standard. After centrifugation at 10000g, 10 min, 4 °C, the supernatants are kept at 4 °C for immediate analysis or placed at –80 °C in case of postponement of the analysis. Controls (t_0 and t_{final}) in triplicate are prepared by incubation of the internal standard with microsomes denatured by acetonitrile. The LC-MS used for this study is a Waters® Acquity I-Class/Xevo TQD, equipped with a Waters® Acquity BEH C18 column, 50 × 2.1 mm, 1.7 µm. The mobile phases are (A) ammonium acetate 10 mM and (B) acetonitrile with 0.1% formic acid. The injection volume is 1 µL and the flow rate is 600

$\mu\text{L}/\text{min}$. The chromatographic analysis, total duration of 4 min, is made with the following gradient: $0 < t < 0.2$ min, 2% (B); $0.2 < t < 2$ min, linear increase to 98% (B); $2 < t < 2.5$ min, 98% (B); $2.5 < t < 2.6$ min, linear decrease to 2% (B); $2.6 < t < 4$ min, 2% (B). 8-Bromo-6-chloro-3-nitro-2-(phenylsulfonylmethyl)imidazo [1,2-*a*]pyridine is used as internal standard. The quantification of each compound is obtained by converting the average of the ratios of the analyte/internal standard surfaces to the percentage of consumed product. The ratio of the control at t_0 corresponds to 0% of product consumed. The calculation of the half-life ($t_{1/2}$) of each compound in the presence of microsomes is done according to the equation: $t_{1/2} = \frac{\ln(2)}{k}$. Where k is the first-order degradation constant (the slope of the logarithm of compound concentration versus incubation time). The intrinsic clearance *in vitro* (Cl_{int} expressed in $\mu\text{L}/\text{min}/\text{mg}$) is calculated according to the equation: $Cl_{\text{int}} = \frac{\text{dose}}{AUC_{\infty}}/[\text{microsomes}]$. Where dose is the initial concentration of product in the sample, AUC_{∞} is the area under the concentration-time curve extrapolated to infinity and $[\text{microsomes}]$ is the microsome concentration expressed in $\text{mg}/\mu\text{L}$.

Plasma protein binding procedure—The plasma doped with the tested compound is incubated at 37 °C in triplicate in one of the compartments of the insert, the other compartment containing a phosphate buffer solution at pH 7.2. After stirring for 4 h at 300 rpm, a 25 μL aliquot of each compartment is taken and diluted; the dilution solution is adapted to obtain an identical matrix for all the compartments after dilution. In parallel, the reprocessing of a plasma doped but not incubated will allow to evaluate the recovery of the study. The LC-MS used for this study is a Waters® Acquity I-Class/Xevo TQD, equipped with a Waters® Acquity BEH C18 column, 50×2.1 mm, 1.7 μm . The mobile phases are (A) ammonium acetate 10 mM and (B) acetonitrile with 0.1% formic acid. The injection volume is 1 μL and the flow rate is 600 $\mu\text{L}/\text{min}$. The chromatographic analysis, total duration of 4 min, is made with the following gradient: $0 < t < 0.2$ min, 2% (B); $0.2 < t < 2$ min, linear increase to 98% (B); $2 < t < 2.5$ min, 98% (B); $2.5 < t < 2.6$ min, linear decrease to 2% (B); $2.6 < t < 4$ min, 2% (B). Carbamazepine, oxazepam, warfarine and diclofenac are used as reference drugs and Propranolol is used as internal standard. The unbound fraction (f_u) is calculated according to the following formula: $f_u = \frac{A_{\text{Plasma, 4h}} - A_{\text{PBS, 4h}}}{A_{\text{Plasma, 4h}}} \times 100$. The

percentage of recovery is calculated according to the following formula:

$$\% \text{ Recovery} = \frac{(V_{\text{PBS}} \times A_{\text{PBS, 4h}}) + (V_{\text{Plasma}} \times A_{\text{Plasma, 4h}})}{V_{\text{Plasma}} \times A_{\text{Plasma, 0h}}}$$

Where A is the ratio of the area under peak of the studied molecule and the area under peak of the internal standard (propranolol 200 nM). V is the volume of solution present in the compartments ($V_{\text{PBS}} = 350 \mu\text{L}$ and $V_{\text{plasma}} = 200 \mu\text{L}$).

Supplementary Material

Refer to Web version on PubMed Central for supplementary material.

Acknowledgments

A. Fairlamb and S. Wyllie are supported by funding from the Wellcome Trust (WT105021). J. Pedron thanks the Université Paul Sabatier de Toulouse and the Région Occitanie/Pyrénées-Méditerranée for PhD funding. C. Piveteau from Institut Pasteur de Lille, C. Bijani from Laboratoire de Chimie de Coordination de Toulouse and the mass spectrometry team of the Institut de Chimie de Toulouse are also acknowledged for their support, respectively for pharmacokinetics, NMR and HRMS experiments.

Abbreviations

NTR	Nitroreductase
SAR	Structure-Activity Relationship
rt	room temperature
NBS	N-bromosuccinimide
AIBN	Azobisisobutyronitrile
THF	Tetrahydrofuran
MW	Microwaves
DMF	N,N-Dimethylformamide
Ar.	Argon
NHE	Normal Hydrogen Electrode
IC50	half maximal inhibitory concentration
CC50	half maximal cytotoxic concentration
TBAPF6	Tetrabutylammonium hexafluorophosphate;
SCE	Saturated Calomel Electrode
GC	Glassy Carbon
E°	standard redox potential
E°_{exp}	standard experimental redox potential
E°_{calc}	standard calculated redox potential
HRMS	High-resolution mass spectrometry
NMR	Nuclear Magnetic Resonance
VL	Visceral leishmaniasis
HAT	Human African Trypanosomiasis

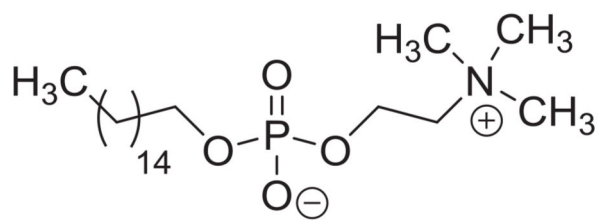
References

- [1]. Pace D. Leishmaniasis. *J Infect.* 2014; 69:S10–S18. DOI: 10.1016/j.jinf.2014.07.016 [PubMed: 25238669]
- [2]. Büscher P, Cecchi G, Jamonneau V, Priotto G. Human African trypanosomiasis. *Lancet.* 2017; 390:2397–2405. DOI: 10.1016/S0140-6736(17)31510-6 [PubMed: 28673422]
- [3]. http://www.who.int/neglected_diseases/diseases/en/
- [4]. World Health Organization. updated 04/2017 <http://www.who.int/mediacentre/factsheets/fs375/en/>
- [5]. World Health Organization. updated 01/2017 <http://www.who.int/mediacentre/factsheets/fs259/en/>
- [6]. Zulfiqar B, Shelper TB, Avery VM. Leishmaniasis drug discovery: recent progress and challenges in assay development. *Drug Discov Today.* 2017; 22:1516–1531. DOI: 10.1016/j.drudis.2017.06.004 [PubMed: 28647378]
- [7]. Ponte-Sucre A, Gamarro A, Dujardin JC, Barrett MP, Lopez-Vélez R, Garcia-Hernández R, Pountain AW, Mwenechanya R, Papadopoulou B. Drug resistance and treatment failure in leishmaniasis: a 21st century challenge. *PLoS Neglected Trop Dis.* 2017; 11doi: 10.1371/journal.pntd.0006052
- [8]. Field MC, Horn D, Fairlamb AH, Ferguson MAJ, Gray DW, Read KD, De Rycker M, Torrie LS, Wyatt PG, Wyllie S, Gilbert IH. Anti-trypanosomatid drug discovery: an ongoing challenge and a continuing need. *Nat Rev Microbiol.* 2017; 15:217–231. DOI: 10.1038/nrmicro.2016.193 [PubMed: 28239154]
- [9]. Patterson S, Wyllie S, Norval S, Stojanovski L, Simeons FRC, Auder JL, Osuna-Cabello M, Read KD, Fairlamb AH. The anti-tubercular drug delamanid as a potential oral treatment for visceral leishmaniasis. *eLife.* 2016; 5:e09744.doi: 10.7554/eLife.09744 [PubMed: 27215734]
- [10]. Ang WC, Jarrad AM, Cooper MA, Blaskovich MAT. Nitroimidazoles: molecular fireworks that combat a broad spectrum of infectious diseases. *J Med Chem.* 2017; 60:7636–7657. DOI: 10.1021/acs.jmedchem.7b00143 [PubMed: 28463485]
- [11]. DNDi. updated 12/2017 <https://www.dndi.org/diseases-projects/portfolio/>
- [12]. Mesu VKBK, Kalonji WM, Bardonneau C, Mordt OV, Blesson S, Simon F, Delhomme S, Bernhard S, Kuziena W, Lubaki JF, Vuvu SL, et al. Oral fexinidazole for late-stage African *Trypanosoma brucei gambiense* trypanosomiasis: a pivotal multicentre, randomised, non-inferiority trial. *Lancet.* 2018; :144–154. DOI: 10.1016/S0140-6736(17)32758-7
- [13]. Patterson S, Wyllie S. Nitro drugs for the treatment of trypanosomatid diseases: past, present, and future prospects. *Trends Parasitol.* 2014; 30:289–298. DOI: 10.1016/j.pt.2014.04.003 [PubMed: 24776300]
- [14]. Wyllie S, Patterson S, Stojanovski L, Simeons FRC, Norval S, Kime R, Read KD, Fairlamb AH. The anti-trypanosome drug fexinidazole shows potential for treating visceral leishmaniasis. *Sci Transl Med.* 2012; 4:119re1.doi: 10.1126/scitranslmed.3003326
- [15]. Verhaeghe P, Rathelot P, Rault S, Vanelle P. Convenient preparation of original vinylic chlorides with antiparasitic potential in quinoline series. *Lett Org Chem.* 2006; 3:891–897. DOI: 10.2174/157017806779467997
- [16]. Paloque L, Verhaeghe P, Casanova M, Castera-Ducros C, Dumètre A, Mbatchi L, Hutter S, Kraiem-M'Rabet M, Laget M, Remusat V, Rault S, et al. Discovery of a new antileishmanial hit in 8-nitroquinoline series. *Eur J Med Chem.* 2012; 54:75–86. DOI: 10.1016/j.ejmech.2012.04.029 [PubMed: 22608675]
- [17]. Kieffer C, Cohen A, Verhaeghe P, Hutter S, Castera-Ducros C, Laget M, Remusat V, Kraiem M'Rabet M, Rault S, Rathelot P, Azas N, et al. Looking for new antileishmanial derivatives in 8-nitroquinolin-2(1*H*)-one series. *Eur J Med Chem.* 2015; 92:282–294. DOI: 10.1016/j.ejmech.2016.09.029 [PubMed: 25559208]
- [18]. Kieffer C, Cohen A, Verhaeghe P, Paloque L, Hutter S, Castera-Ducros C, Laget M, Rault S, Valentin A, Rathelot P, Azas N, et al. Antileishmanial pharmacomodulation in 8-nitroquinolin-2(1*H*)-one series. *Bioorg Med Chem.* 2015; 23:2377–2386. DOI: 10.1016/j.bmc.2015.03.064 [PubMed: 25846065]
- [19]. Andreev VP, Nizhnik YP. Reaction of 2,4-dibromoquinoline with hydrogen chloride. *Russ J Org Chem.* 2002; 38:137–138. DOI: 10.1023/A:1015331531268

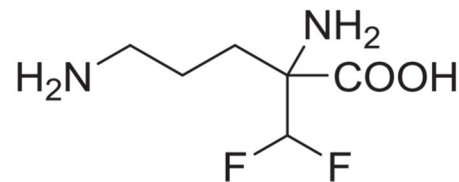
- [20]. O'Brien NJ, Brzozowski M, Wilson DJD, Deady LW, Abbott BM. Synthesis and biological evaluation of substituted 3-anilinoquinolin-2(1*H*)-ones as PDK1 inhibitors. *Bioorg Med Chem.* 2014; 22:3781–3790. DOI: 10.1016/j.bmc.2014.04.037 [PubMed: 24856302]
- [21]. Zaragoza F, Stephensen H, Peschke B, Rimvall K. 2-(4-Alkylpiperazin-1-yl) quinolines as a new class of Imidazole-free Histamine H₃ Receptor Antagonists. *J Med Chem.* 2005; 48:306–311. DOI: 10.1021/jm031028z [PubMed: 15634025]
- [22]. Zubatyuk RI, Gorb L, Shishkin OV, Qasim M, Leszczynski J. Exploration of density functional methods for one-electron reduction potential of nitrobenzenes. *J Comput Chem.* 2010; 31:144–150. DOI: 10.1002/jcc.21301 [PubMed: 19422001]
- [23]. Uchimiya M, Gorb L, Isayev O, Qasim MM, Leszczynski J. One-electron standard reduction potentials of nitroaromatic and cyclic nitramine explosives. *Environ Pollut.* 2010; 158:3048–3053. DOI: 10.1016/j.envpol.2010.06.033 [PubMed: 20656388]
- [24]. Torreele E, Bourdin Trunz B, Tweats D, Kaiser M, Brun R, Mazué G, Bray MA, Pécoul B. Fexinidazole – a new oral nitroimidazole drug candidate entering clinical development for the treatment of sleeping sickness. *PLoS Neglected Trop Dis.* 2010; 4:e923.doi: 10.1371/journal.pntd.0000923
- [25]. Wyllie S, Patterson S, Fairlamb AH. Assessing the essentiality of *Leishmania donovani* nitroreductase and its role in nitro drug activation. *Antimicrob Agents Chemother.* 2013; 57:901–906. DOI: 10.1128/AAC.01788-12 [PubMed: 23208716]
- [26]. Wyllie S, Roberts AJ, Norval S, Patterson S, Foth BJ, Berriman M, Read KD, Fairlamb AH. Activation of bicyclic nitro-drugs by a novel nitroreductase (NTR2) in *Leishmania*. *PLoS Pathog.* 2016; 12:e1005971.doi: 10.1371/journal.ppat.1005971 [PubMed: 27812217]
- [27]. Purohit V, Basu AK. Mutagenicity of nitroaromatic compounds. *Chem Res Toxicol.* 2000; 13:673–692. DOI: 10.1021/tx000002x [PubMed: 10956054]
- [28]. Rosenkranz EJ, McCoy EC, Mermelstein R, Rosenkranz HS. Evidence for the existence of distinct nitroreductases in *Salmonella typhimurium*: roles in mutagenesis. *Carcinogenesis.* 1982; 3:121–123. DOI: 10.1093/carcin/3.1.121 [PubMed: 7039852]
- [29]. Buschini A, Ferrarini L, Franzoni S, Galati S, Lazzaretti M, Mussi F, Northfleet de Albuquerque C, Araujo Domingues Zucchi T-M, Poli P. Genotoxicity reevaluation of three commercial nitroheterocyclic drugs: nifurtimox, benznidazole and metronidazole. *J Parasitol Res.* 2009; 2009doi: 10.1155/2009/463575
- [30]. Misani F, Bogert NT. The search for superior drugs for tropical diseases; further experiments in the quinolone group. *J Org Chem.* 1945; 10:458–463. DOI: 10.1021/jo01181a012 [PubMed: 21004582]
- [31]. Moores IG, Smalley RK, Suschitzky H. Alkaline Hydrolysis of 2-(Trifluoromethyl)imidazo[4,5-f] and -[4,5-h] quinolines. *J Fluorine Chem.* 1982; 20:573–580. DOI: 10.1016/S0022-1139(00)82282-4
- [32]. Ishikawa M, Kikkawa I. Studies on quinoline derivatives. IV. *Yakugaku Zasshi.* 1955; 75:36–39. DOI: 10.1248/yakushi1947.75.1_36
- [33]. Patil VV, Shankarling GS. Steric-hindrance-induced Regio- and Chemo-selective Oxidation of Aromatic amines. *J Org Chem.* 2015; 80:7876–7883. DOI: 10.1021/acs.joc.5b00582 [PubMed: 26212905]
- [34]. Johnson OH, Hamilton CS. Syntheses in the quinoline series. III. The nitration of 2-chloro-4-methylquinoline and the preparation of some 2-hydroxy-4-methyl-8-(dialkylaminoalkyl)-aminoquinolines. *J Am Chem Soc.* 1941; 63:2867–2869. DOI: 10.1021/ja01856a003
- [35]. Todorov AR, Wirtanen T, Helaja J. Photoreductive removal of *O*-Benzyl groups from Oxyarene *N*-Heterocycles assisted by *O*-Pyridine-pyridone Tautomerism. *J Org Chem.* 2017; 82:13756–13767. DOI: 10.1021/acs.joc.7b02775 [PubMed: 29135249]
- [36]. Rosenhauer E. Über Reaktionen von *N*-Alkyl- α -metylen-chinolanen, I.: Diazo-Kupplung der Metylenbase in neutraler Lösung. (Mitbearbeitet von O. Dannhofer.). *Eur J Inorg Chem.* 1924; 57:1291–1294. DOI: 10.1002/cber.19240570813
- [37]. Hashimoto T. Amyostatic poisons. VIII. Syntheses of alkyl derivatives of 3-amino-3,4-dihydrocarbostyryl and diamino-3,4-dihydrocarbostyryl. *Yakugaku Zasshi.* 1955; 75:340–342. DOI: 10.1248/yakushi1947.75.3_340

- [38]. Mislow K, Koepfli JB. The synthesis of potential Antimalarials. Some 2-substituted 8-(3-Diethylaminopropylamino)-quinolines. *J Am Chem Soc.* 1946; 68:1553–1556. DOI: 10.1021/ja01212a050 [PubMed: 20994976]
- [39]. Frisch, MJ, Trucks, GW, Schlegel, HB, Scuseria, GE, Robb, MA, Cheeseman, JR, Scalmani, G, Barone, V, Mennucci, B, Petersson, GA, Nakatsuji, H. , et al. Gaussian 09, Revision D.01. Gaussian, Inc; Wallingford CT: 2013.
- [40]. Zhao Y, Truhlar DG. The M06 suite of density functionals for main group thermochemistry, thermochemical kinetics, noncovalent interactions, excited states, and transition elements: two new functionals and systematic testing of four M06-class functionals and 12 other functionals. *Thero Chem Acc.* 2008; 120:215–241. DOI: 10.1007/s00214-007-0310-x
- [41]. Tomasi J, Mennucci B, Cammi R. Quantum mechanical continuum solvation models. *Chem Rev.* 2005; 105:2999–3093. DOI: 10.1021/cr9904009 [PubMed: 16092826]
- [42]. Kelly CP, Cramer CJ, Truhlar DG. Aqueous solvation free energies of Ions and Ion-water Clusters based on an accurate value for the absolute aqueous solvation free energy of the Proton. *J Phys Chem B.* 2006; 110:16066–16081. DOI: 10.1021/jp063552y [PubMed: 16898764]
- [43]. Zhang C, Bourgeade-Delmas S, Alvarez AF, Valentin A, Hemmert C, Gornitzka H. Synthesis, characterization, and antileishmanial activity of neutral *N*-heterocyclic carbenes gold(I) complexes. *Eur J Med Chem.* 2018; 143:1635–1643. DOI: 10.1016/j.ejmech.2017.10.060 [PubMed: 29133045]
- [44]. Mosman TJ. Rapid colorimetric assay for cellular growth and survival: application to proliferation and cytotoxicity assays. *J Immunol Meth.* 1983; 65:55–63. DOI: 10.1016/0022-1759(83)90303-4
- [45]. Da Luz RI, Vermeersch M, Dujardin JC, Cos P, Maes L. Vitro sensitivity testing of Leishmania clinical field Isolates: Preconditioning of promastigotes Enhances Infectivity for macrophage host cells. *Antimicrob Agents Chemother.* 2009; 53:5197–5203. DOI: 10.1128/AAC.00866-09 [PubMed: 19752271]
- [46]. Goyard S, Segawa H, Gordon J, Showalter M, Duncan R, Turco SJ, Beverley SM. An in vitro system for developmental and genetic studies of *Leishmania donovani* phosphoglycans. *Mol Biochem Parasitol.* 2003; 130:31–42. DOI: 10.1016/S0166-6851(03)00142-7 [PubMed: 14550894]
- [47]. Wyllie S, Patterson S, Fairlamb AH. Assessing the essentiality of Leishmania donovani nitroreductase and its role in nitro drug activation. *Antimicrob Agents Chemother.* 2013; 57:901–906. DOI: 10.1128/AAC.01788-12 [PubMed: 23208716]
- [48]. Wyllie S, Roberts AJ, Norval S, Patterson S, Foth BJ, Berriman M, Read KD, Fairlamb AH. Activation of bicyclic nitro-drugs by a novel nitroreductase (NTR2) in Leishmania. *PLoS Pathog.* 2016; 12:e1005971. doi: 10.1371/journal.ppat.1005971 [PubMed: 27812217]
- [49]. Wyllie S, Patterson S, Stojanovski L, Simeons FRC, Norval S, Kime R, Read KD, Fairlamb AH. The anti-trypanosome drug fexinidazole shows potential for treating visceral leishmaniasis. *Sci Transl Med.* 2012; 4:119re1. doi: 10.1126/scitranslmed.3003326
- [50]. Baltz T, Baltz D, Giroud C, Crockett J. Cultivation in a semi-defined medium of animal infective forms of *T. brucei*, *T. equiperdum*, *T. evansi*, *T. rhodesiense* and *T. gambiense*. *EMBO J.* 1985; 4:1273–1277. [PubMed: 4006919]
- [51]. Räs B, Iten M, Grether-Bühler Y, Kaminsky R. The AlamarBlue® Blue assay to determine drug sensitive of African trypanosome (*T. brucei rhodesiense* and *T. brucei gambiense*) in vitro. *Acta Trop.* 1997; 68:139–147. DOI: 10.1016/S0001-706X(97)00079-X [PubMed: 9386789]
- [52]. Guillon J, Cohen A, Nath Das R, Boudot C, Gueddouda N, Moreau S, Ronga L, Savrimoutou S, Rubio S, Amaziane S, Dassonville-Klimpt A, et al. Design, synthesis, and antiprotozoal evaluation of new 2,9-bis[(substituted-aminomethyl)phenyl]-1,10-phenanthroline derivatives. *Chem Biol Drug Des.* 2018; :1–22. DOI: 10.1111/cbdd.13164
- [53]. Greig N, Wyllie S, Patterson S, Fairlamb AH. *FEBS J.* 2009; 276:376–386. [PubMed: 19076214]
- [54]. Wyllie S, Foth BJ, Kelner A, Sokolova AY, Berriman M, Fairlamb AH. *J Antimicrob Chemother.* 2016; 71:625–634. [PubMed: 26581221]
- [55]. Jones DC, Hallyburton I, Stojanovski L, Read KD, Frearson JA, Fairlamb AH. *Biochem Pharmacol.* 2010; 80:1478–1486. [PubMed: 20696141]

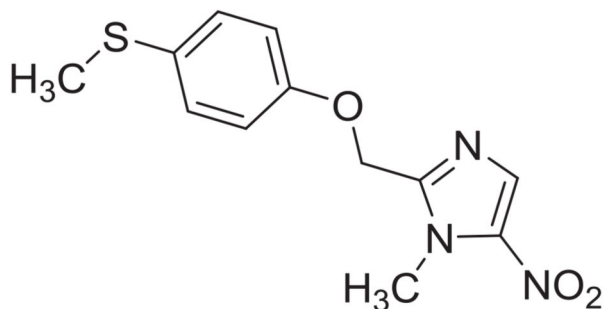
- [56]. De Méo M, Laget M, Di Giorgio C, Guiraud H, Botta A, Castegnaro M, Duménil G. Optimization of the Salmonella/mammalian microsome assay for urine mutagenesis by experimental designs. *Mutat Res.* 1996; 340:51–65. [PubMed: 8692182]
- [57]. Perdry H, Gutzkow KB, Chevalier M, Huc L, Brunborg G, Boutet-Robinet E. Validation of Gelbond® high-throughput alkaline and Fpg-modified comet assay using a linear mixed model. *Environ Mol Mutagen.* 2018; doi: 10.1002/em.22204



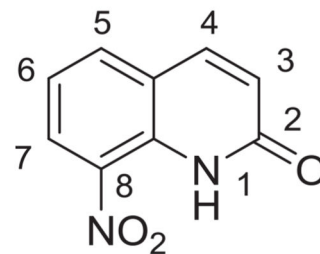
Miltefosine
Antileishmanial Drug



Eflornithine
Antitrypanosomal Drug



Fexinidazole
Antikinetoplastid Drug Candidate



8-nitroquinolin-2[1*H*]-one
Antileishmanial Hit

Fig. 1.
Structures of the antikinetoplastid drugs miltefosine and eflornithine, drug-candidate fexinidazole and antileishmanial hit 8-nitroquinolin-2(1*H*)-one.

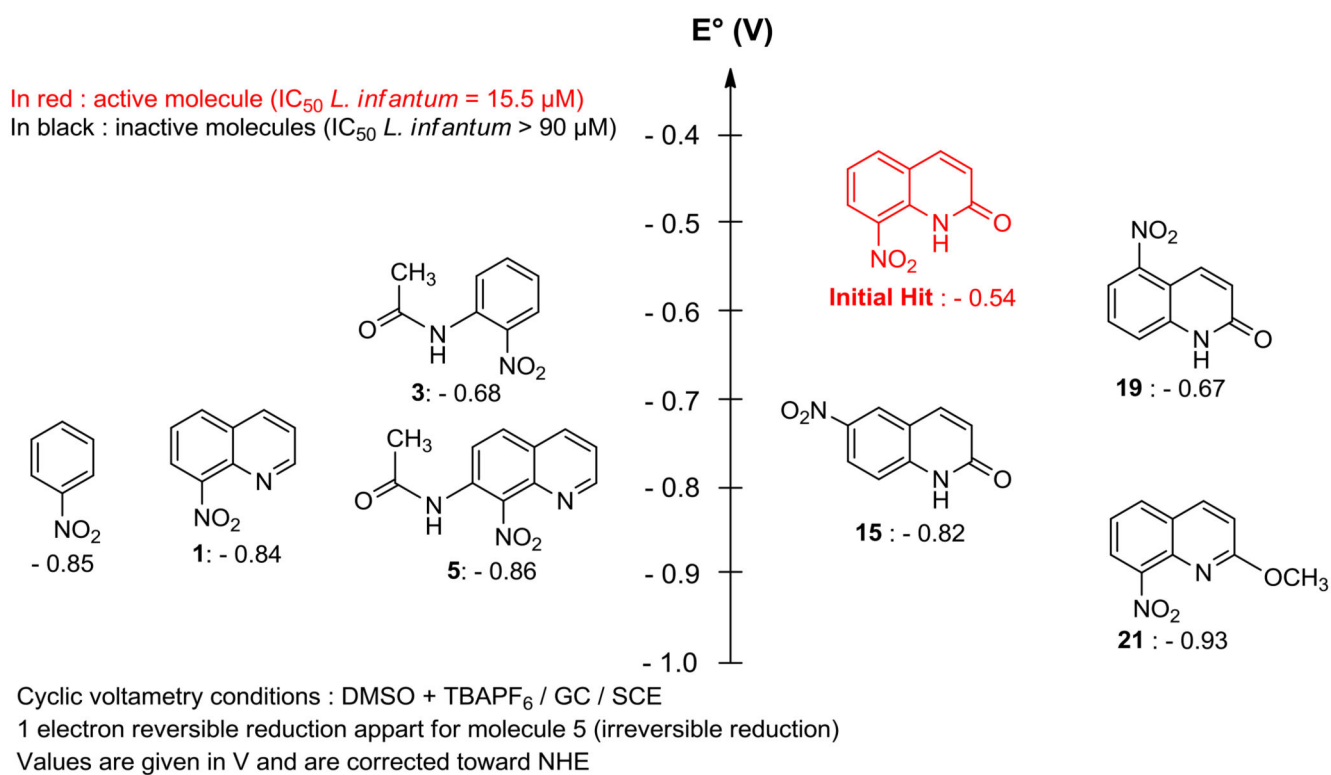


Fig. 2.
 The 8-nitroquinolin-2(1*H*)-one pharmacophore presented a characteristic high redox potential value.

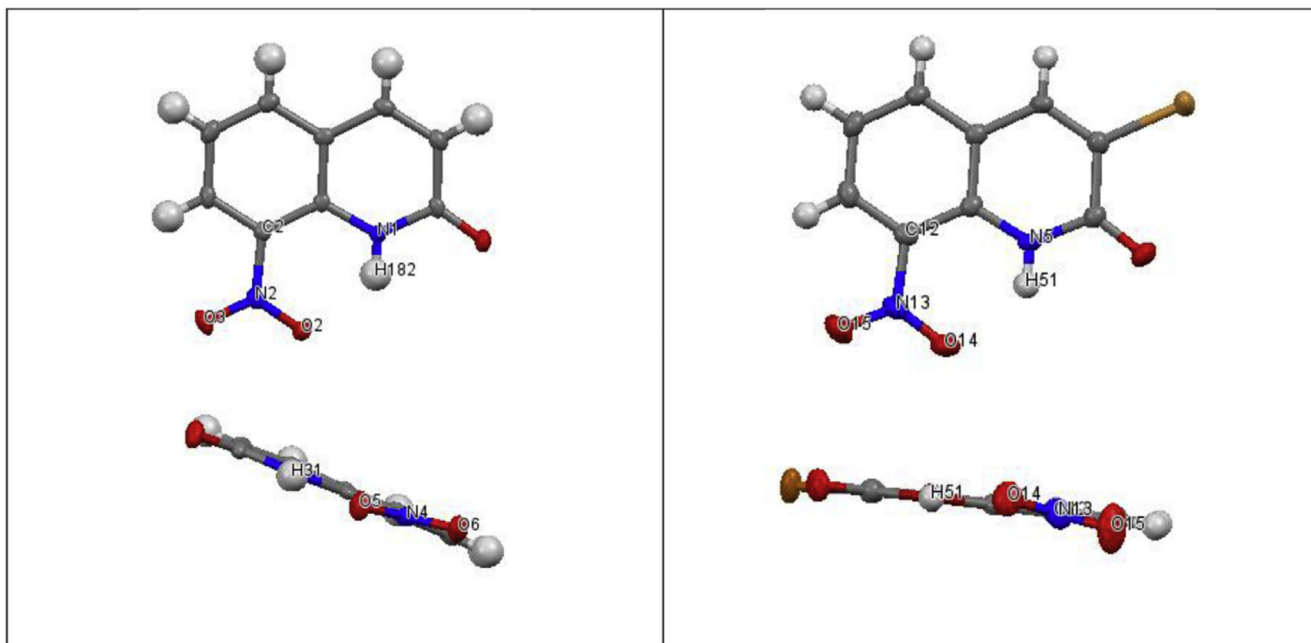


Fig. 3. X-ray structures of initial hit and new hit **22** presenting an intramolecular hydrogen bond between the lactam function and the nitro group (Initial hit: N-H distance = 0.89 Å, H-O distance = 2.01 Å, N-H-O angle = 129°; Hit **22**: N-H distance = 0.84 Å, H-O distance = 2.01 Å, N-H-O angle = 131°).

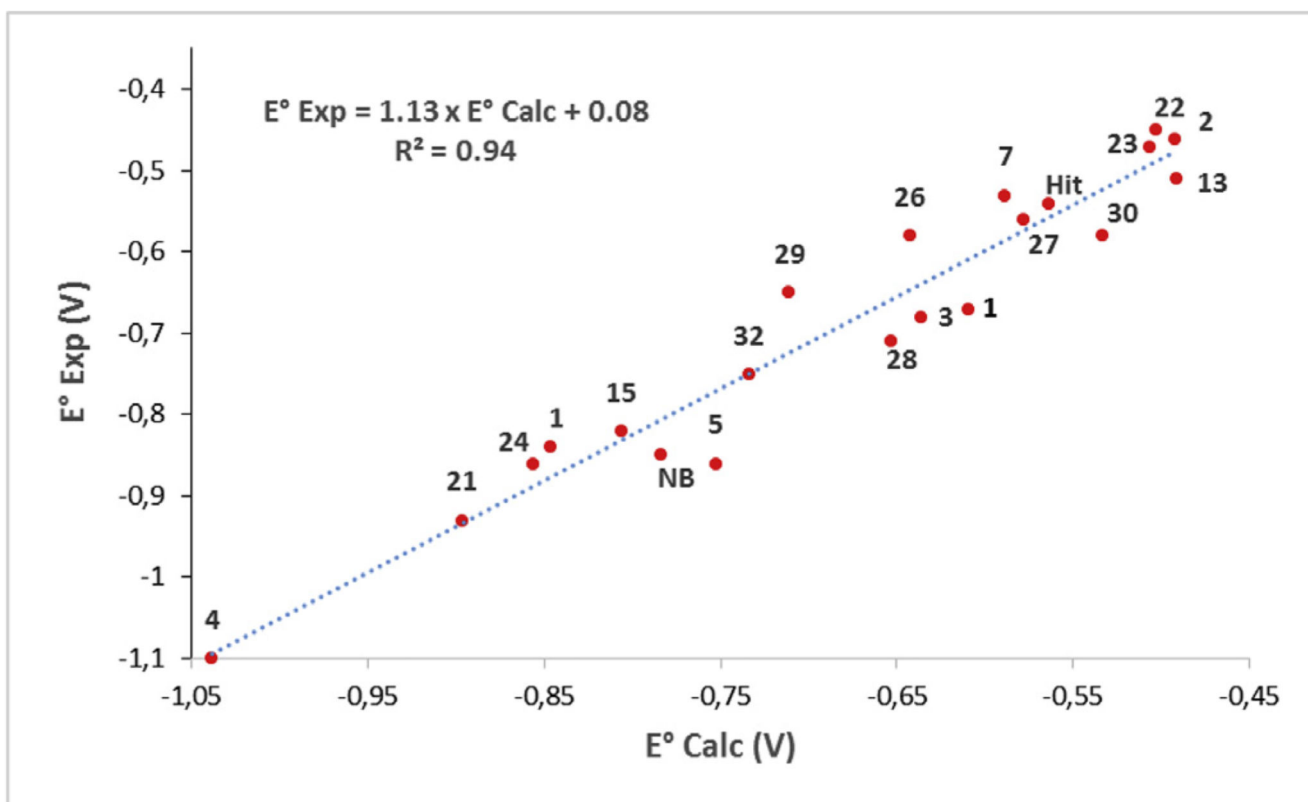


Fig. 4. Correlation between theoretical and experimental standard redox potential of nitroquinolines.

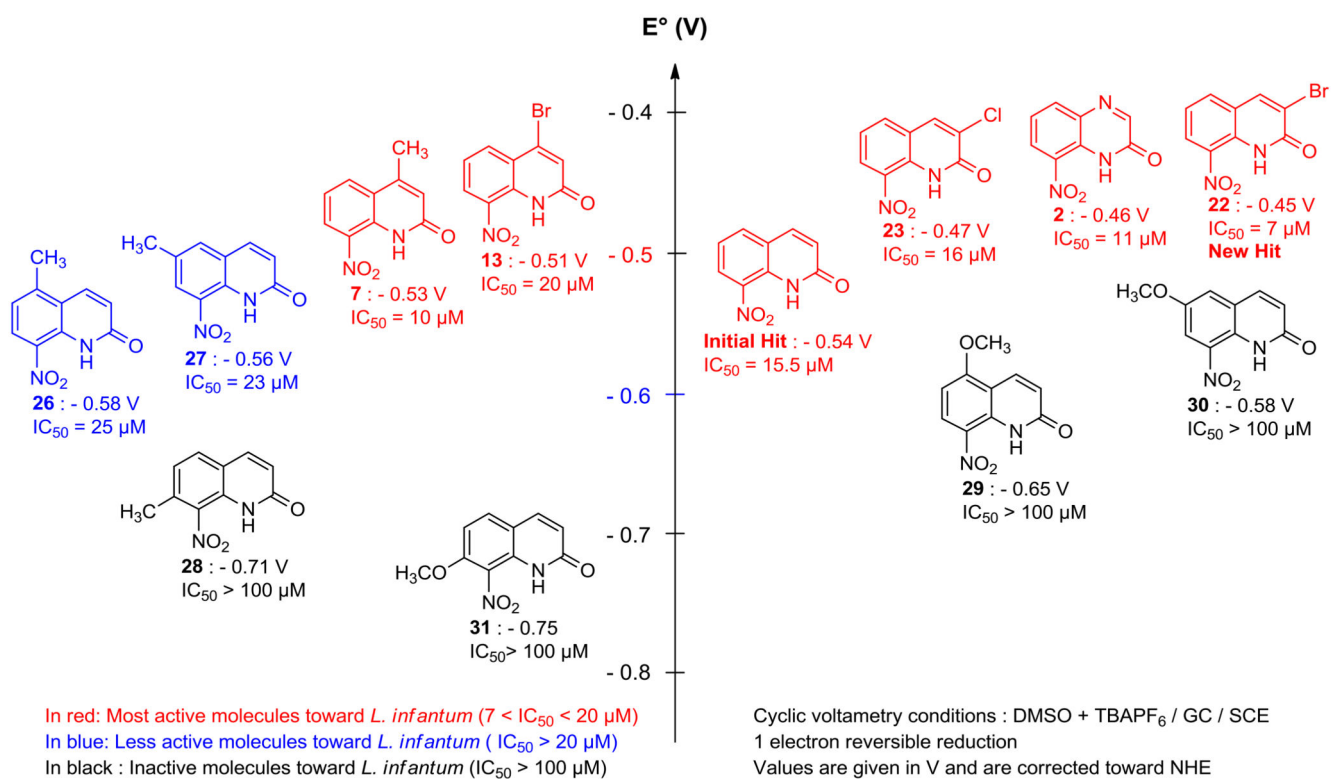


Fig. 5. Modulation of the redox potential of the 8-nitroquinolin-2 [1H]-one pharmacophore. Mode of action studies, genotoxicity evaluation and preliminary pharmacokinetic properties of **22**.

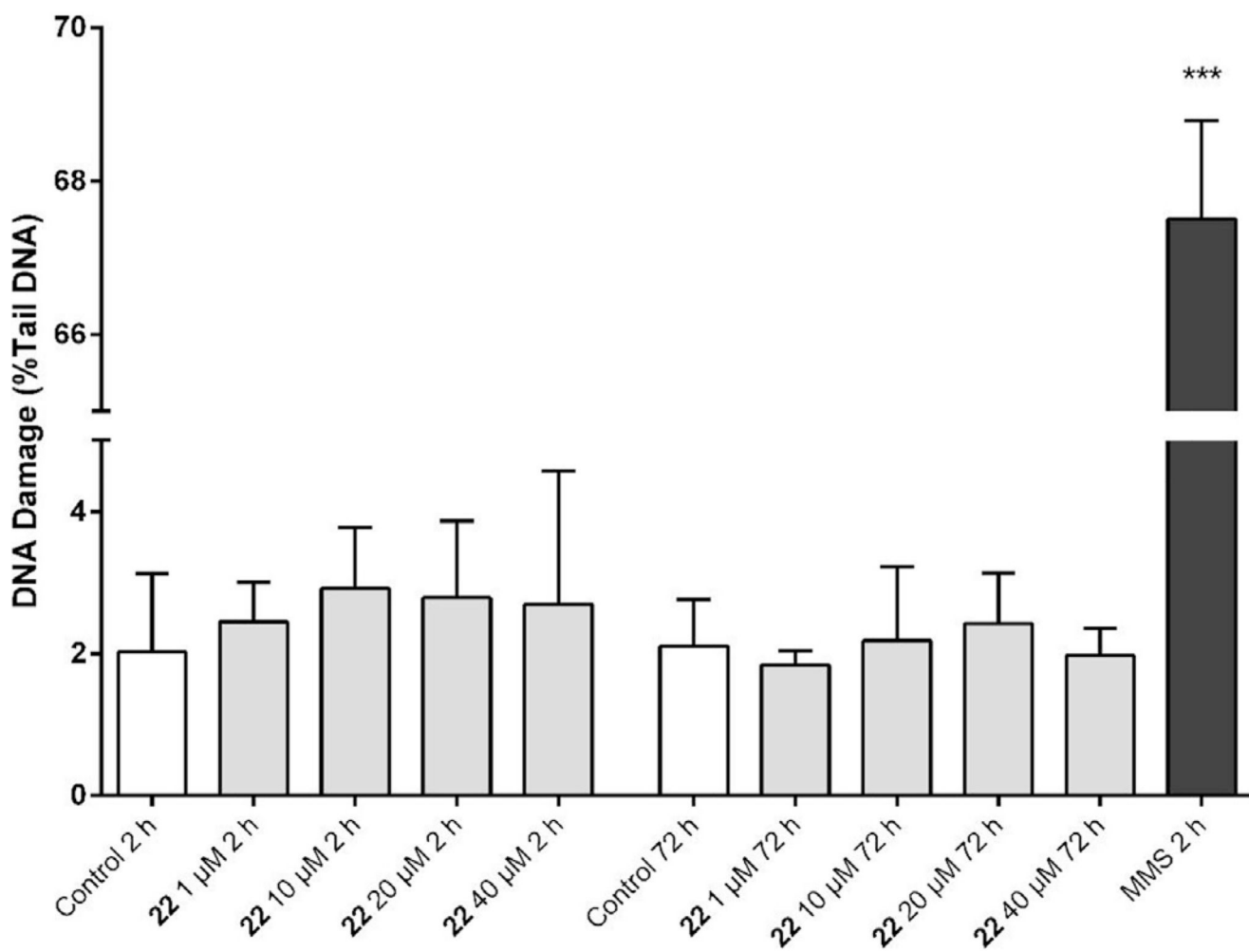
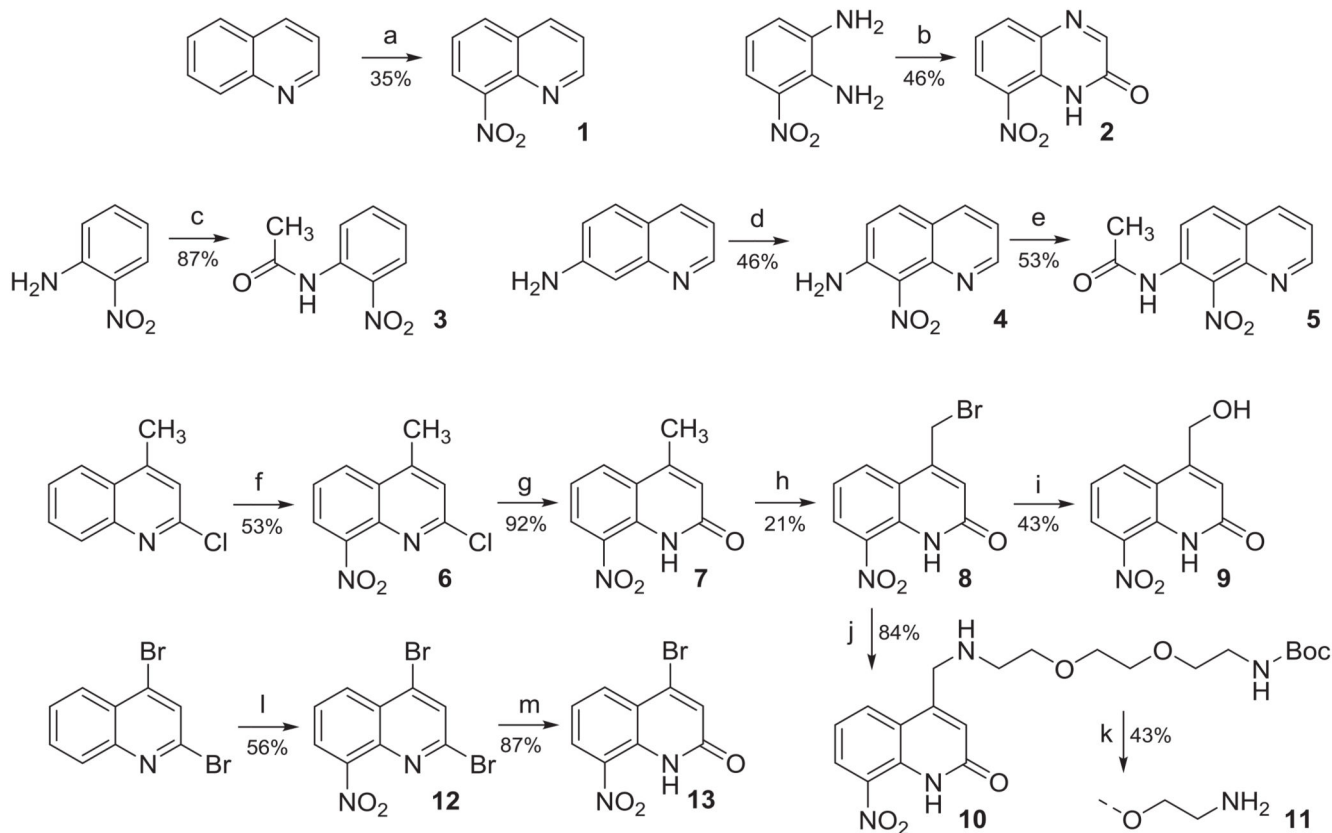
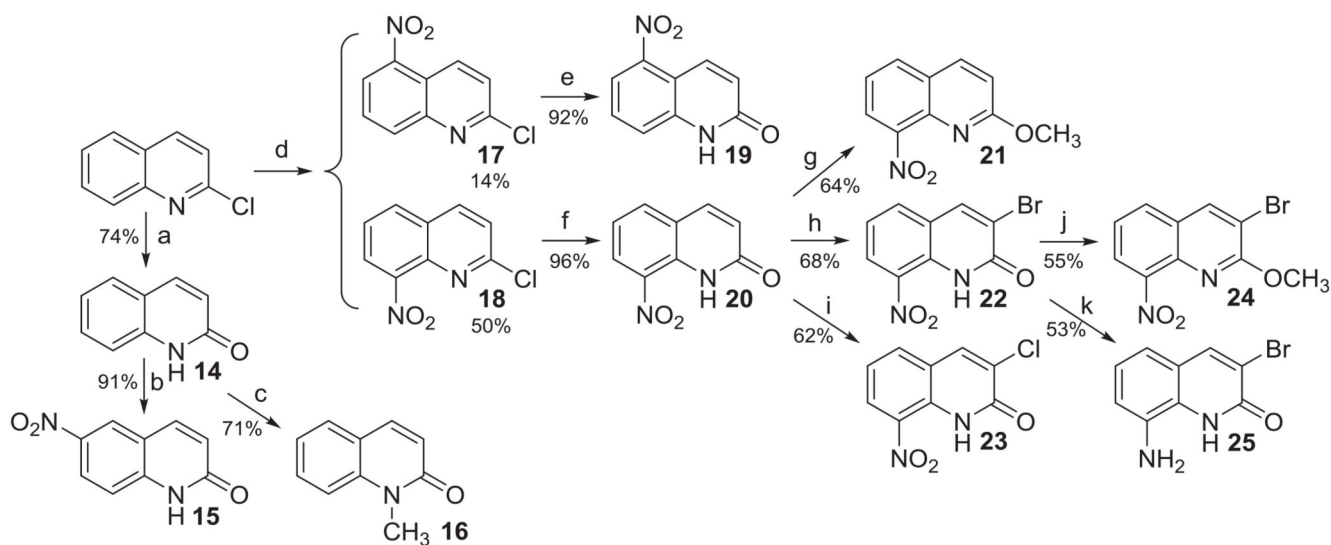


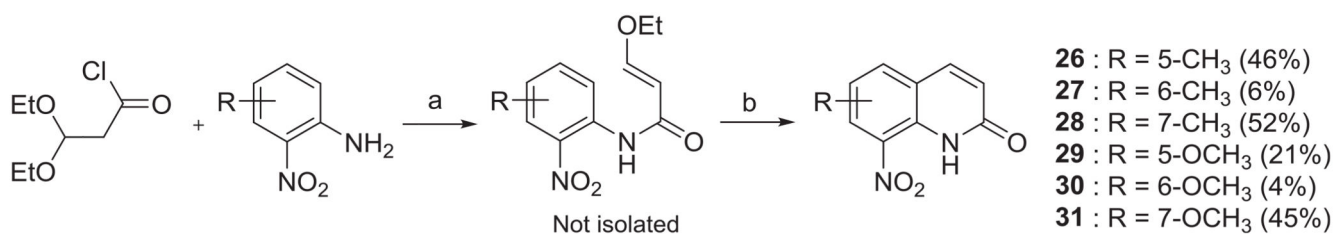
Fig. 6.
Results of the comet assay for hit compound **22**.
Positive control = MMS = 1 mM methylmethanesulfonate.

**Scheme 1.**

Synthetic routes for the preparation of compounds 1–13. (a) H_2SO_4 , HNO_3 , rt, 1 h; (b) glyoxylic acid, EtOH, 80 °C, 6 h; (c) CH_3COOH , Ac_2O , 120 °C, 3 h; (d) H_2SO_4 , HNO_3 , rt, 4 h; (e) CH_3COOH , Ac_2O , 120 °C, 24 h; (f) H_2SO_4 , HNO_3 , rt, 3 h; (g) CH_3CN , HClO_4 , 100 °C, 24 h; (h) NBS, AIBN, CCl_4 , 80 °C, 24 h; (i) NaOH, $\text{H}_2\text{O}/\text{THF}$, 50 °C, 24 h; (j) $\text{NH}_2(\text{CH}_2\text{CH}_2\text{O})_2\text{CH}_2\text{CH}_2\text{NHBoc}$, THF, 50 °C, 24 h; (k) HCl (5 N in isopropanol), rt, 4 h; (l) H_2SO_4 , HNO_3 , rt, 2 h; (m) CH_3CN , HClO_4 , MW, 100 °C, 1 h.

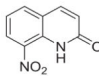
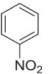
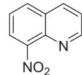
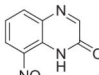
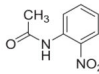
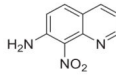
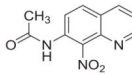
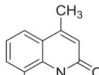
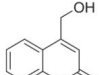
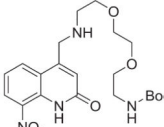
**Scheme 2.**

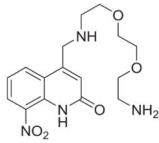
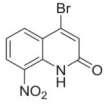
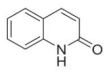
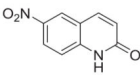
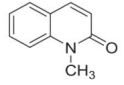
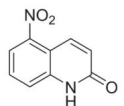
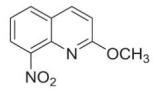
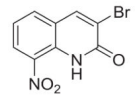
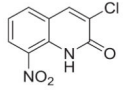
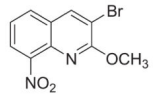
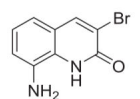
Preparation of compounds 14–25 from 2-chloroquinoline. (a) CH_3CN , HClO_4 , $100\text{ }^\circ\text{C}$, 72 h; (b) H_2SO_4 , HNO_3 , rt, 1 h; (c) DMF , K_2CO_3 , CH_3I , $80\text{ }^\circ\text{C}$, 48 h; (d) H_2SO_4 , HNO_3 , rt, 2 h; (e) CH_3CN , HClO_4 , $100\text{ }^\circ\text{C}$, 72 h; (f) CH_3CN , HClO_4 , $100\text{ }^\circ\text{C}$, 72 h; (g) Ar., DMF , NaH , CH_3I , rt, 24 h; (h) NaBrO_3 , HBr , $100\text{ }^\circ\text{C}$, 5 h; (i) NaClO_3 , HCl , $100\text{ }^\circ\text{C}$, 45 min; (j) Ar., DMF , NaH , CH_3I , rt, 24 h; (k) EtOH , SnCl_2 , $80\text{ }^\circ\text{C}$, 3 h.

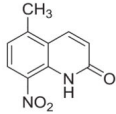
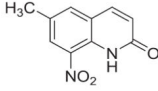
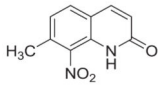
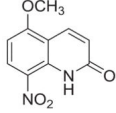
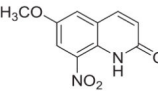
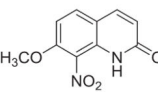
**Scheme 3.**

Preparation of compounds 26–31 from nitroanilines substrates. (a) CH₂Cl₂, Pyridine, rt, 24 h;
 (b) H₂SO₄, rt, 3–4 h.

Table 1
Reduction potentials, calculated LogP, anti-kinetoplastid activity and cytotoxicity of the synthesized nitroaromatic compounds 1–31.

Molecule	Structure	E° (V/NHE) ^a	LogP ^b	<i>L. infantum</i> axenic amastigote IC ₅₀ (μM)	<i>T. brucei brucei</i> trypomastigote IC ₅₀ (μM)	HepG2 Cytotoxicity CC ₅₀ (μM)
Initial hit		- 0.54	1.54	15.5 ± 0.5	23.4 ± 5.7	164 ± 28
Nitro-benzene (NB)		- 0.85	1.91	>100 ^d	>50 ^d	>100 ^d
1		- 0.84	2.07	>100 ^d	17.9 ± 1.8	>100 ^d
2		- 0.46	1.2	11.0 ± 2.1	7.3 ± 0.8	125 ± 19
3		- 0.68	1.15	>100 ^d	>50 ^d	>100 ^d
4		- 1.1	1.89	>100 ^d	>50 ^d	>100 ^d
5		- 0.86 ^c	1.31	>100 ^d	10.8 ± 1.4	>100 ^d
7		- 0.53	2.05	10.2 ± 1.0	20.9 ± 8.9	110 ± 9
9		–	–	23.4 ± 4.8	38.3 ± 6.1	>100 ^d
10		–	–	>100 ^d	2.5 ± 1.8	>100 ^d

Molecule	Structure	E° (V/NHE) ^a	LogP ^b	<i>L. infantum</i> axenic amastigote IC ₅₀ (μM)	<i>T. brucei brucei</i> trypomastigote IC ₅₀ (μM)	HepG2 Cytotoxicity CC ₅₀ (μM)
11		-	-	>100 ^d	7.6 ± 1.8	>100 ^d
13		- 0.51	1.86	20.3 ± 5.0	5.5 ± 1.3	60 ± 2
14		- 1.86 ^b	-	>100 ^d	>50 ^d	>100 ^d
15		- 0.82	1.54	>100 ^d	2.3 ± 0.6	>100 ^d
16		-	-	>100 ^d	>50 ^d	>100 ^d
19		- 0.67	1.54	>100 ^d	>50 ^d	>100 ^d
21		- 0.93	2.51	88.8 ± 13.0	28.5 ± 8.1	>100 ^d
22		- 0.45	2.36	7.1 ± 1.5	1.9 ± 0.4	92 ± 13
23		- 0.47	2.2	16.0 ± 0.9	1.2 ± 0.2	85 ± 4
24		- 0.86	-	>6.2 ^e	0.4 ± 0.1	>6.2 ^e
25		-	-	>50 ^d	>50 ^d	>100 ^d

Molecule	Structure	E° (V/NHE) ^a	LogP ^b	<i>L. infantum</i> axenic amastigote IC ₅₀ (μM)	<i>T. brucei brucei</i> trypomastigote IC ₅₀ (μM)	HepG2 Cytotoxicity CC ₅₀ (μM)
26		- 0.58	2.05	25.2 ± 3.7	29.1 ± 4.7	>100 ^d
27		- 0.56	2.05	23.0 ± 5.0	2.1 ± 0.8	>100 ^d
28		- 0.71	2.05	>100 ^d	>50 ^d	>100 ^d
29		- 0.65	1.38	>100 ^d	>50 ^d	>100 ^d
30		- 0.58	1.38	>100 ^d	>50 ^d	>100 ^d
31		- 0.75	1.38	>100 ^d	>50 ^d	>100 ^d
Doxorubicin ^f		-	-	-	-	0.2 ± 0.02
Amphotericin B ^g		-	-	0.06 ± 0.001	-	5.5 ± 0.25
Miltefosine ^g		-	-	0.8 ± 0.2	-	85 ± 8.8
Fexinidazole ^{g,h}		-	-	3.4 ± 0.8	0.4 ± 0.2	>200 ^c
Suramin ^h		-	-	-	0.02 ± 0.009	>100 ^c
Eflornithine ^h		-	-	-	15.8 ± 2.1	>100 ^c

^aCyclic voltammetry conditions: DMSO/TBAPF₆, SCE/GC, 1 electron reversible reduction, values are given in V versus NHE.

^bWeighted logP were computed with Marvin[®] (ChemAxon).

^cIrreversible reduction.

^dThe IC₅₀ or CC₅₀ value was not reached at the highest tested concentration.

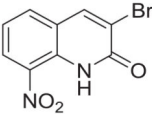
^eThe product could not be tested at higher concentrations due to a poor solubility in aqueous medium.

^fDoxorubicin was used as a cytotoxic reference drug.

^gAmphotericin B, Miltefosine and Fexinidazole were used as antileishmanial reference drugs.

^hFexinidazole, Suramin and Eflornithine were used as anti-*Trypanosoma brucei* reference drugs.

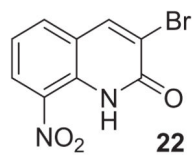
Table 2
Complementary *in vitro* biological evaluations done on hit compound 22.

<i>In vitro</i> studies	
	
	Compound 22
Cytotoxicity: CC ₅₀ THP1 (μM) ^a	72 ± 6
IC ₅₀ <i>L. donovani</i> intramacrophagic amastigotes (μM) ^b	18 ± 2
IC ₅₀ <i>L. donovani</i> promastigotes wild type strain (μM)	5.9 ± 0.12
IC ₅₀ <i>L. donovani</i> promastigotes NTR1 over-expressing strain (μM)	0.47 ± 0.02
IC ₅₀ <i>L. donovani</i> promastigotes NTR2 over-expressing strain (μM)	4.6 ± 0.12
IC ₅₀ <i>T. b. brucei</i> trypomastigotes wild type strain (μM)	17.7 ± 1.0
IC ₅₀ <i>T. b. brucei</i> trypomastigotes NTR1 over-expressing strain (μM)	3.9 ± 0.1
Microsomal stability: T _{1/2} (min)	>40
Binding % to human albumin	92

^aReference compounds: Amphotericin B CC₅₀ = 3.6 ± 0.7 μM; Miltefosine CC₅₀ > 40 μM; Fexinidazole CC₅₀ > 62.5 μM.

^bReference compounds: Amphotericin B IC₅₀ = 0.4 μM; Miltefosine IC₅₀ = 5.4 μM; Fexinidazole IC₅₀ > 50 μM.

Table 3
Ames test results for hit compound 22.



	0.25 mM	2.5 mM
TA97a + S9 mix	Positive	Positive
TA98 + S9 mix	Positive	Positive
TA100 + S9 mix	Positive	Positive
TA102 + S9 mix	Negative	Positive

Benzo [a]pyrene was used as a positive control.